CoA Note No. 11

RESTRICTED

THE COLLEGE OF AERONAUTICS

CRANFIELD

LONGITUDINAL STABILITY CHARACTERISTICS AND DAMPING IN PITCH OF DELTA WINGS

by

W. B. McCARTER, M.A.Sc. (Toronto)

NOTE NO. 11

JULY, 1954.

THE COLLEGE OF AERONAUTICS

CRANFIELD

Note on the longitudinal stability characteristics and damping in pitch of delta wings at subsonic, transonic and supersonic speeds*

-by-

W.B. McCarter, M.A.Sc. (Toronto)

SUMMARY AND CONCLUSIONS

The usual technique of longitudinal stability analysis is adopted but particular attention is paid to those elements that contribute to damping. The cases of two delta plan form aircraft of 45° and 60° sweep angle are considered and, in the light of the best available data, their derivatives and the coefficients of the stability quartics are obtained for a range of Mach numbers including the transonic range. An analysis is made of the damping of the short period oscillation in each case and this is compared with a requirement to damp to half-amplitude in less than one cycle. The results are dependent on estimates and assumptions that cannot be regarded as completely reliable in the absence of experimental data, and quasi-static derivatives are used in cases where frequency effects should properly be included; but the broad implications of the results are probably acceptable. They suggest that the damping of the tailless 45° delta is inadequate at transonic speeds, whilst that of the tailless 60° delta may be adequate for values of the relative density parameter, $\mu_1 = W/\frac{1}{2}\rho\bar{c}g$, less than about 200. Various methods of improving the damping are discussed briefly, and some simple examples of response are included.

---

* Part of thesis submitted at the College of Aeronautics, June, 1953.

CONTENTS

LIST OF FIGURES

1. Introduction

The delta planform is regarded as particularly well suited to flight at transonic speeds since the advantages of high sweep, low aspect ratio, and thin section can all be exploited to minimise the effects of compressibility on the aerodynamic coefficients and derivatives. Structural advantages are also claimed.

The longitudinal damping characteristics of the tailless delta at transonic and supersonic speeds are however suspect and require investigation. In this paper the usual approach to longitudinal stability analysis is adopted but particular attention is paid to those elements that contribute to the damping. The cases of two delta plan form aircraft of 45° and 60° sweep angle are considered and, in the light of the best available data, their derivatives and the coefficients of the stability quartics are obtained for a range of Mach numbers including the transonic range. An analysis is made of the damping of the short period mode in each case, and this is compared with a requirement to damp to half amplitude in less than one cycle. Some simple response calculations given in the appendix illustrate the more important conclusions. The analysis is approximate and, in particular, quasi-steady values of the derivatives are used although it is clear for the cases considered that the frequency may be an important parameter in the transonic range of Mach numbers. Nevertheless the broad implications of the conclusions are probably valid and it is believed that the detailed results of the analysis will have considerable intrinsic interest.

2. Notation

2.1. Axes and velocity components

x,z	rectangular Cartesian right handed co-ordinates with origin at the aircraft centre of gravity; x forward along the axis of symmetry, z vertically downwards
X,Z	forces along the x,z axes, respectively (lb.)
M	pitching moment (ft.lb.)
u,w	increment of velocity in directions x,z respectively (ft./sec.)
q	angular velocity about pitching axis (rad./sec.)

θ increment in angle of pitch

γ angle between aircraft flight path and horizontal (rad.)

V undisturbed (steady) true airspeed (ft./sec.)

α wing angle of attack

B moment of inertia about pitching axis through centre of gravity

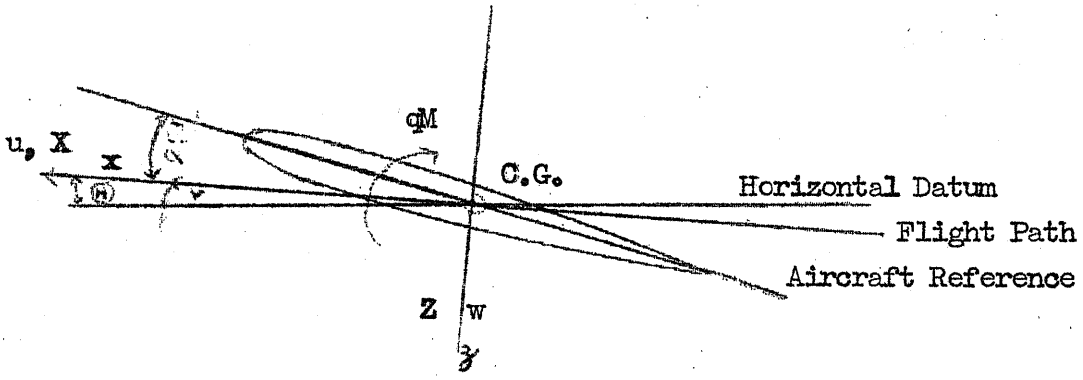

WIND AXES

2.2. Aircraft geometry

S wing area $= b\bar{c} = \frac{1}{2}bc_o(1+\lambda)$ $(ft.^2)$

λ taper ratio $= c_t/c_o$

c_t tip chord (ft.)

c_o root chord (ft.)

b wing span (ft.)

$\bar{c}$ standard mean chord (S.M.C.) $= \frac{1}{2}c_o(1+\lambda) = \frac{3}{4} \cdot \frac{\bar{\bar{c}}}{1-\lambda/(1+\lambda)^2}$

$\bar{\bar{c}}$ mean aerodynamic chord (M.A.C.) $= \frac{2}{3}c_o\left(1+\lambda - \frac{\lambda}{1+\lambda}\right)$
$= \frac{4}{3}\bar{c}\left[1 - \frac{\lambda}{(1+\lambda)^2}\right]$

x_o distance of C.G. from apex (ft.)

$\bar{x}$ distance of leading edge of M.A.C. from apex
$= \bar{y}\tan\Lambda = \frac{1}{3}c_o\frac{(1-\lambda)(1+2\lambda)}{1+\lambda}$

$\bar{y}$ spanwise position of M.A.C. and S.M.C. from aircraft centre line $= \frac{b}{6}\frac{1+2\lambda}{1+\lambda} = \frac{c_o}{3}\frac{(1-\lambda)(1+2\lambda)}{\tan\Lambda\,(1+\lambda)}$

Λ sweep of leading edge

h position of C.G. on M.A.C. in fraction of M.A.C.
$= \frac{x_o-\bar{x}}{\bar{\bar{c}}} = \frac{x_o}{\bar{\bar{c}}} - \frac{1+\lambda-2\lambda^2}{2(1+\lambda+\lambda^2)}$

A aspect ratio $= \frac{2b}{c_o(1+\lambda)} = 4 \cot\Lambda \left[\frac{1-\lambda}{1+\lambda}\right] = 3 \cot\Lambda_{c/4} \left[\frac{1-\lambda}{1+\lambda}\right]$

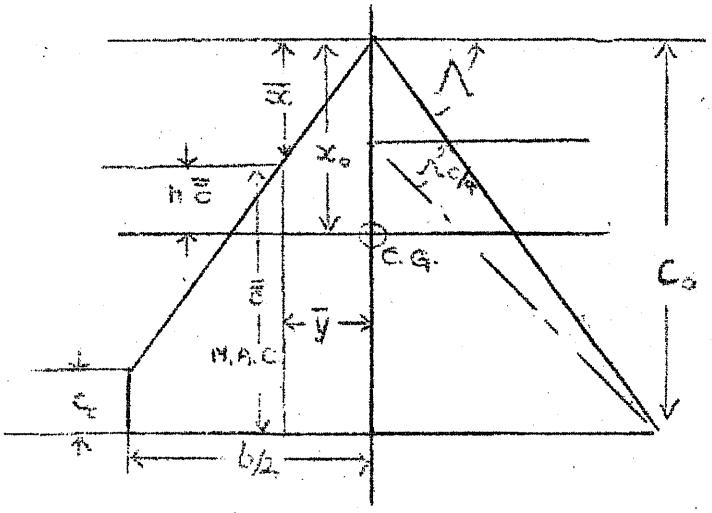

2.3. Fundamental notation

a	wing angle of attack (degrees or radians)
η	control deflection (degrees or radians), a downward deflection is positive (a positive control angle normally gives rise to a negative moment)
ϵ	downwash angle (radians)
g	acceleration due to gravity (ft/sec.^{2})
t	time (seconds)
W	aircraft weight (lb.wt.)
m	aircraft mass $= W/g$ (lb.mass)
M_1	Mach number $= V/a$
a	speed of sound in air (ft/sec.)
ρ	density of air (slug/ft.^{3})
C_m	pitching moment/$(\frac{1}{2}\rho V^2 S\bar{c})$

Suffix t refers to a tail. Further notation will be defined in the text. It may be noted that the revisions suggested by Bryant and Gates[20] to stability notation have been adopted here with the object of presenting an example of their effect. Appendix I summarises the resulting relation between the derivatives as here defined and as defined in other sources.

3. The linearised equations of motion for dynamic longitudinal stability

The basic assumptions made are:

1. The equations as developed apply to small perturbations from horizontal flight.
2. Aeroelastic distortion effects are considered negligible.
3. Cross-coupling derivatives between the lateral and longitudinal modes are neglected.
4. Wind axes are used.
5. Since power-operated controls are most likely with the type of aircraft considered only stick-fixed stability is considered.
6. The variations of density and speed of sound with height are neglected. As shown in Ref. 18 these variations at high Mach numbers can have important effects on the phugoid motion but the effects on the short period motion are negligible. Since we are here primarily concerned with the latter it is felt that the neglect of these variations is justified.

The dimensional equations of motion in the usual notation as developed under the above assumptions are:[1,2]

$$\left.\begin{aligned} m\dot{u} + mg\theta - X_u u - X_w w - X_q q - X_{\dot{w}}\dot{w} &= X_o \\ m(\dot{w} - V\dot{\theta}) - Z_u u - Z_w w - Z_q q - Z_{\dot{w}}\dot{w} &= Z_o \\ B\ddot{\theta} - M_u u - M_w w - M_q q - M_{\dot{w}}\dot{w} &= M_o \\ q &= \dot{\theta} \end{aligned}\right\} \quad \ldots\ldots\ldots\ldots(1)$$

In non-dimensional form these equations become

$$\left.\begin{aligned} \left(\frac{d\hat{u}}{d\hat{t}} - x_u\hat{u}\right) - \left(x_w\hat{w} + \frac{x_{\dot{w}}}{\mu}\cdot\frac{d\hat{w}}{d\hat{t}}\right) + \left(C_L\theta - \frac{x_q}{\mu}\cdot\frac{d\theta}{d\hat{t}}\right) &= x_o \\ - z_u\hat{u} - \left[z_w\hat{w} + \left(\frac{z_{\dot{w}}}{\mu} - 1\right)\frac{d\hat{w}}{d\hat{t}}\right] - \left(\frac{z_q}{\mu} + 1\right)\frac{d\theta}{d\hat{t}} &= z_o \\ - \frac{\mu}{i_B}\cdot m_u\hat{u} - \left(\frac{\mu}{i_B}m_w + \frac{m_{\dot{w}}}{i_B}\frac{d\hat{w}}{d\hat{t}}\right) + \left(\frac{d^2\theta}{d\hat{t}^2} - \frac{m_q}{i_B}\frac{d\theta}{d\hat{t}}\right) &= m_o \end{aligned}\right\} \quad \ldots(2)$$

where the aerodynamic effects of deflected control angle to trim may be included in the appropriate derivatives and coefficients.

Here, it should be noted that the unit of time τ is defined by

$$\tau = m/\tfrac{1}{2}\rho SV ,$$

so that $\hat{t} = t/\tau = t\frac{1}{2}\rho SV/m$,

and the relative density is

$$\mu_1 = m/\tfrac{1}{2}\rho S\bar{\bar{c}} ,$$

where $\bar{\bar{c}}$ is the aerodynamic mean chord.

Also

$$x_u = X_u/\tfrac{1}{2}\rho SV, \text{ etc.},$$
$$x_{\dot{w}} = X_{\dot{w}}/\tfrac{1}{2}\rho S\bar{\bar{c}}, \text{ etc.},$$
$$x_q = X_q/\tfrac{1}{2}\rho SV\bar{\bar{c}}, \text{etc.},$$
$$m_u = M_u/\tfrac{1}{2}\rho SV\bar{\bar{c}}, \text{etc.},$$
$$m_{\dot{w}} = M_{\dot{w}}/\tfrac{1}{2}\rho S\bar{\bar{c}}^2$$
$$m_q = M_q/\tfrac{1}{2}\rho SV\bar{\bar{c}}^2,$$
$$x_o = X_o/\tfrac{1}{2}\rho V^2 S, \text{ etc.},$$
$$m_o = \mu M_o/i_B\tfrac{1}{2}\rho V^2 S\bar{\bar{c}} ,$$

the notation is otherwise standard.

4. The Stability Quartic

For the complementary function, we set $x_o = z_o = m_o = 0$, and following traditional lines we assume solutions of the form:

$$\hat{u} = k_1 e^{\lambda\hat{t}}, \quad \hat{w} = k_2 e^{\lambda\hat{t}}, \quad \theta = k_3 e^{\lambda\hat{t}} ,$$

where k_1, k_2, k_3 and λ are constants, which may be complex, and where one of the k's may be taken to be unity.

Substitution of these expressions into equations (2) and division by $e^{\lambda\hat{t}}$ results in three equations for these four constants.

$$\left.\begin{aligned} &(\lambda - x_u)k_1 - \left(x_w + \frac{x_{\dot{w}}}{\mu_1}\lambda\right)k_2 + \left(C_L\theta - \frac{x_q}{\mu_1}\lambda\right)k_3 = 0 \\ &-z_u k_1 - \left[z_w + \left(\frac{z_{\dot{w}}}{\mu_1} - 1\right)\lambda\right]k_2 - \left(\frac{z_q}{\mu_1} + 1\right)\lambda k_3 = 0 \\ &-\frac{\mu}{i_B}m_u k_1 - \left(\frac{\mu}{i_B}m_w + \frac{m_{\dot{w}}}{i_B}\lambda\right)k_2 + \left(\lambda^2 - \frac{m_q}{i_B}\lambda\right)k_3 = 0 \end{aligned}\right\} \quad (3)$$

The compatibility condition is then

$$\begin{vmatrix} \lambda - x_u & -\left(x_w + \frac{x_{\dot{w}}}{\mu_1}\lambda\right) & C_L\theta - \frac{x_q}{\mu}\lambda \\ -z_u & -\left[z_w + \left(\frac{z_{\dot{w}}}{\mu_1} - 1\right)\lambda\right] & -\left(\frac{z_q}{\mu_1} + 1\right)\lambda \\ -\frac{\mu_1}{i_B}m_u & -\left(\frac{\mu_1}{i_B}m_w + \frac{m_{\dot{w}}}{i_B}\lambda\right)\lambda^2 & -\frac{m_q}{i_B}\lambda \end{vmatrix} = 0 \qquad ..(4)$$

Expansion of this determinant gives a quartic in λ of the form:

$$A\lambda^4 + B\lambda^3 + C\lambda^2 + D\lambda + E = 0 \qquad .....(5)$$

where

$$\left.\begin{aligned} A &= 1 - \frac{z_{\dot{w}}}{\mu_1} \\ B &= z_w + \left(\frac{z_{\dot{w}}}{\mu_1} - 1\right)\left(x_u + \frac{m_q}{i_B}\right) - \left(\frac{z_q}{\mu_1} + 1\right)\frac{m_{\dot{w}}}{i_B} - z_w\frac{x_{\dot{w}}}{\mu_1} \\ C &= z_w\left(x_u + \frac{m_q}{i_B}\right) + \left(\frac{z_{\dot{w}}}{\mu_1} - 1\right)\left(\frac{x_q}{i_B}m_u - x_u\frac{m_q}{i_B}\right) \\ &\quad + \left(\frac{z_q}{\mu_1} + 1\right)\left(\frac{m_{\dot{w}}}{i_B}x_u - \frac{\mu_1 m_w}{i_B} - \frac{x_{\dot{w}}}{i_B}m_u\right) \\ &\quad + z_u\left(\frac{x_{\dot{w}}}{\mu_1}\cdot\frac{m_q}{i_B} - x_w - \frac{m_{\dot{w}}}{i_B}\frac{x_q}{\mu_1}\right) \\ D &= z_w\left(\frac{x_q}{i_B}m_u - x_u\frac{m_q}{i_B}\right) + \left(\frac{z_{\dot{w}}}{\mu_1} - 1\right)\left(-C_L\mu_1\frac{m_u}{i_B}\right) \\ &\quad + \left(\frac{z_q}{\mu_1} + 1\right)\left(x_u\mu_1\frac{m_{\dot{w}}}{i_B} - x_w\mu_1\frac{m_u}{i_B}\right) + z_u\left(\frac{m_{\dot{w}}}{i_B}C_L + \frac{m_q}{i_B}x_w - \frac{x_q}{i_B}m_w\right) \end{aligned}\right\} \qquad (6)$$

$$E = \frac{\mu_1}{i_B}C_L\left(m_w z_u - z_w m_u\right) .$$

The roots of the longitudinal stability quartic are, in general, two complex pairs, one pair corresponding to a short period oscillation and the other pair to an oscillation of considerably longer period which are subsequently referred to as the 'short period' and 'long period' modes of motion of the aircraft.

Thus the roots may be written $\lambda_{1,2} = r_{1,2} + is_{1,2}$ where the subscripts 1 and 2 refer to the short and long period motion respectively.

A first approximation to the roots can be taken as:

$$\left.\begin{aligned} r_1 &= -\frac{B}{2A} \quad , \quad s_1 = \sqrt{\frac{C}{A} - \left(\frac{B}{2A}\right)^2} \\ r_2 &= -\tfrac{1}{2}\left(\frac{D}{C} - \frac{BE}{C^2}\right) , \quad s_2 = \sqrt{\frac{E}{C} - \frac{1}{4}\left(\frac{D}{C} - \frac{BE}{C^2}\right)^2} \end{aligned}\right\} \quad (7)$$

These roots can be improved until the following expressions are satisfied to the desired number of decimal places:

$$2r_1 + 2r_2 = -B ,$$

$$(r_1^2 + s_1^2)(r_2^2 + s_2^2) = E .$$

The mode of oscillation corresponding to a particular pair of roots is stable if the real part is negative, and unstable if the real part is positive. The necessary and sufficient conditions for stability are that all coefficients of the quartic and in addition Routh's discriminant

$$R = BCD - AD^2 - B^2E$$

must be of the same sign.

The period and damping of the two oscillatory modes are given by:

$$\text{Period} = 2\pi\tau/s_{1,2} \quad \text{seconds per cycle}$$

$$\text{Time to half amplitude} = (\log_e 2\tau)/r_{1,2} \text{ seconds.}$$

Also of interest is the number of cycles to damp to half amplitude given by

$$\text{Cycles to half amplitude} = \frac{\text{Time to half amplitude}}{\text{period}} = -0.11032\,\frac{s_{1,2}}{r_{1,2}} . \quad (8)$$

When the two pairs of roots are obtained, the determination of k_1, k_2, k_3 corresponding to each root is made by substituting back into any pair of equations (3). The calculation of the complete response of an aircraft to any given disturbance requires a particular integral as well as the complementary function of the stability equations (2). Various well known

techniques are available for this (see, for example Ref. 2).

5. Formulae for the Aerodynamic Derivatives

It is readily shown (see for example, Refs. 2 and 20) that

$$x_u = -M_1\left(\frac{\partial C_D}{\partial M_1}\right)_a - 2C_D \quad * \qquad \ldots\ldots\ldots\ldots(9)$$

$$z_u = -M_1\left(\frac{\partial C_L}{\partial M_1}\right)_a - 2C_L \qquad \ldots\ldots\ldots\ldots(10)$$

$$x_w = C_L - \left(\frac{\partial C_D}{\partial a}\right)_{M_1} \qquad \ldots\ldots\ldots\ldots(11)$$

$$z_w = -C_D - \left(\frac{\partial C_L}{\partial a}\right)_{M_1} \qquad \ldots\ldots\ldots\ldots(12)$$

$$m_u = M_1\left(\frac{\partial C_m}{\partial M_1}\right)_a + 2C_m \qquad \ldots\ldots\ldots\ldots(13)$$

$$= M_1\left(\frac{\partial C_m}{\partial M_1}\right)_a \quad \text{for a trimmed aircraft}$$

$$m_w = \left(\frac{\partial C_m}{\partial a}\right)_{M_1} \qquad \ldots\ldots\ldots\ldots(14)$$

$$x_q = -\frac{\partial C_D}{\partial(q\bar{\bar{c}}/V)} \qquad \ldots\ldots\ldots\ldots(15)$$

$$z_q = -\frac{\partial C_L}{\partial(q\bar{\bar{c}}/V)} \qquad \ldots\ldots\ldots\ldots(16)$$

$$m_q = \frac{\partial C_m}{\partial(q\bar{\bar{c}}/V)} \qquad \ldots\ldots\ldots\ldots(17)$$

$$x_{\dot{w}} = -\frac{\partial C_D}{\partial(\dot{a}\bar{\bar{c}}/V)} \qquad \ldots\ldots\ldots\ldots(18)$$

$$z_{\dot{w}} = -\frac{\partial C_L}{\partial(\dot{a}\bar{\bar{c}}/V)} \qquad \ldots\ldots\ldots\ldots(19)$$

and

$$m_{\dot{w}} = \frac{\partial C_m}{\partial(\dot{a}\bar{\bar{c}}/V)} \qquad \ldots\ldots\ldots\ldots(20)$$

* No account is here taken of any contribution of the propulsive unit

6. Determination of the Aerodynamic Coefficients and Stiffness Derivatives

For these derivatives the control contributions have been neglected.

Drag Coefficient

The drag is assumed to consist of the sum of two parts, the drag at zero lift and that due to lift, and a further subdivision is as follows.-

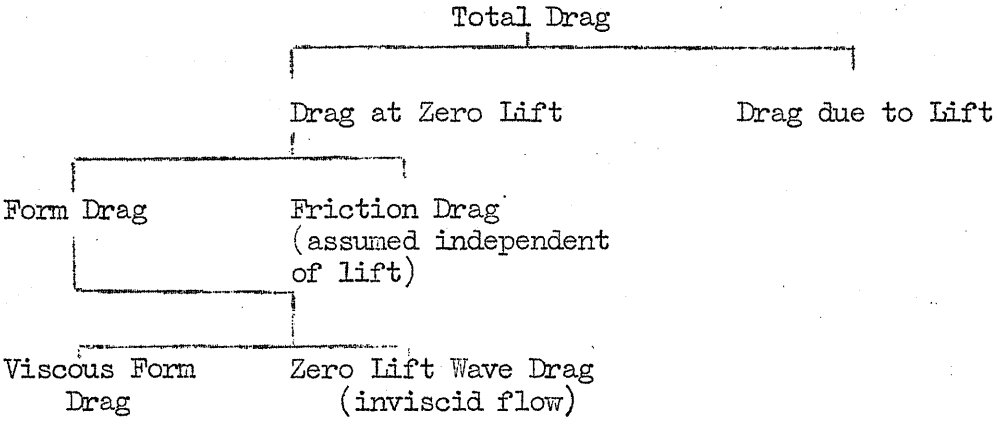

The formula for drag coefficient is then given by:

$$C_D = C_D(o) + KC_L^2 \qquad \text{.....(21)}$$

where $C_D(o)$ is the zero lift drag coefficient

and $$K = \partial C_D / \partial C_L^2 . \qquad \text{.....(22)}$$

For the examples chosen the wing is assumed to have a symmetrical section comparable to the N.A.C.A. 4 digit series with a mean weighted thickness-chord ratio of 6 per cent. That is, where

$$\tau^2 = \frac{\int_o^{b/2} (t/c)^2 c \, dy}{\int_o^{b/2} c \, dy} = 0.0036. \qquad \text{.....(23)}$$

It is further assumed that the maximum thickness is forward at the root and back at the tip relative to a mean position of 0.3c and also that the wing is tapered down in thickness chord ratio from root to tip.

The drag at zero lift has been estimated from test results of ground-launched rocket boosted models[3,4] with

Reynolds number in the range 6.10^6 to 20.10^6. These values were faired into an assumed subsonic drag coefficient of 0.01. An assumed friction drag coefficient of 0.005 was subtracted from the measured zero lift drag coefficients at supersonic speed to give the inviscid flow wave drag C_{D_W} (the viscous form drag was assumed to be negligible at supersonic speeds), and the results fell closely about the curve shown plotted in Figure 1. For that figure μ = Mach angle = $\sin^{-1}(1/M_1) = \cot^{-1}\sqrt{M_1^2-1}$ and Λ is the sweep angle. Figure 2 shows the estimated values of $C_D(o)$ against M_1 for the delta wings of 60° and 45° sweep angle considered. The drag due to lift has been estimated from experimental data for incompressible flow from Ref. 5 and at supersonic speeds from the theory of Robinson in Ref. 6. These results are interpolated at transonic speeds by multiplying the incompressible flow value by $\frac{(\partial C_L/\partial a)_{incomp.}}{(\partial C_L/\partial a)_{comp.}}$. The resulting values are shown plotted in Figure 3.

Lift coefficient

The balance of forces normal to the flight path in undisturbed motion is

$$\tfrac{1}{2}\rho V^2 S C_L = W$$

or

$$C_L M_1^2 = W/(\tfrac{1}{2}\rho a^2 S) = \text{constant.} \quad \ldots\ldots\ldots\ldots (24)$$

The slope of the lift curve has been estimated from the theory of Weissinger in Ref. 7 and modified slightly by experiments as shown in Figure 4. Frequency effects are taken to be negligibly small (see Ref. 8 Chapter 3.3). Figure 5 shows the estimated variations of $(\partial C_L/\partial a)$ with Mach number for the two delta plan forms considered. These curves are based on evidence obtained from Ref. 19.

Aerodynamic centre

Evidence derived from Ref. 7 and some experimental data have been used as a basis for the curves shown in Fig. 6.

Slope of the pitching moment curve at constant Mach number

We have

$$\left(\frac{\partial C_m}{\partial a}\right)_{M_1} = (h-H_o)\left[\left(\frac{\partial C_L}{\partial a}\right)_{M_1} + C_D\right] \qquad \text{.....(25)}$$

hence we can determine $(\partial C_m/\partial a)_{M_1}$ directly from the aerodynamic coefficients already discussed.

Slope of the drag curve at constant Mach number

From equation (20),

$$C_D = C_D(o) + KC_L.$$

Therefore

$$\left(\frac{\partial C_D}{\partial a}\right)_{M_1} = 2KC_L\left(\frac{\partial C_L}{\partial a}\right)_{M_1} \qquad \text{.....(26)}$$

and hence $(\partial C_D/\partial a)_{M_1}$ can also be derived from the relations given above.

Rate of change of lift coefficient with Mach number at constant incidence

If $A = (\partial C_L/\partial a)_{M_1}$

then $C_L = (\partial C_L/\partial a)_{M_1}\, a = Aa$

and

$$\left(\frac{\partial C_L}{\partial M_1}\right)_a = \frac{\partial A}{\partial M_1}a = \frac{C_L}{A}\cdot\frac{\partial A}{\partial M_1} \qquad \text{.....(27)}$$

Rate of change of drag coefficient with Mach number at constant incidence

From equation (20)

$$\left(\frac{\partial C_D}{\partial M_1}\right)_a = \frac{\partial C_D(o)}{\partial M_1} + 2KC_L\left(\frac{\partial C_L}{\partial M_1}\right)_a + C_L^2\frac{\partial K}{\partial M_1}$$

$$= \frac{\partial C_D(o)}{\partial M_1} + \frac{2KC_L^2}{A}\frac{\partial A}{\partial M_1} + C_L^2\frac{\partial K}{\partial M_1} \qquad \text{.....(28)}$$

Rate of change of pitching moment coefficient with Mach number at constant incidence

$$C_m = C_L (h-H_o)$$

$$\left(\frac{\partial C_m}{\partial M_1}\right)_a = C_L \frac{\partial (h-H_o)}{\partial M_1} + (h-H_o) \left(\frac{\partial C_L}{\partial M_1}\right)_a$$

$$= - C_L \frac{\partial H_o}{\partial M_1} + (h-H_o) \frac{C_L}{A} \frac{\partial A}{\partial M_1} \qquad \text{.....(29)}$$

The above relations are sufficient to determine all the stiffness derivatives, that is, x_u, z_u, m_u, x_w, z_w and m_w. These derivatives will be found plotted in the following diagrams Fig. 7 (x_w), Fig. 8 (z_w), Fig. 9 ($-m_w$), Fig. 10 ($-x_u$), Fig. 11 ($-z_u$), Fig. 12 ($-m_u$).

7. Determination of the Damping Derivatives

The force-angular velocity derivative x_q and the force-acceleration derivative $x_{\dot{w}}$ can both be safely neglected since approximately

$$x_q \approx (H_o-h)\, x_w \qquad \text{.....(30)}$$

and

$$x_{\dot{w}} \approx \frac{\partial C_D}{\partial a} (H_o-h) \qquad \text{.....(31)}$$

The remaining damping terms have been estimated using the theory of Multhopp-Garner,[9] Lehrian,[10,11] Mangler,[12,13] Garrick,[14] Ribner and Malve. stuto.[15,16]

Garrick,[14] in reviewing some research on flutter, derived certain analytical results for unsteady incompressible flow past wings of very small aspect ratio based on an extension of the classical theory of R.T. Jones. This analysis is also reviewed in Ref. 9.

According to this theory

$$l(x) = 2\pi\rho V s \dot{\phi} \left[s + (ds/dx)(x-x_o) \right]$$

where $\phi = \theta + a$, and $\dot{\phi} = \dot{\theta} + \dot{a} \approx q + \dot{w}/V$, x is measured in the

direction of the free stream from a datum point, x_o denotes the position of the lateral axis about which the wing is oscillating, $s = s(x)$ denotes the semi-span of a transverse strip of the wing, and $l(x)$ is the lift per unit length in the direction of the free stream.

Substituting

$$s = s(x) = Ax/4$$

$$l(x) = (\pi/8)\rho V\dot{\phi}A^2 (2x^2 - xx_o)$$

Then

$$C_L = \int_o^{2\bar{c}} \frac{l(x)dx}{\frac{1}{2}\rho V^2 S} \quad \text{where} \quad S = A\bar{c}^2$$

$$= 2\pi A\left(\frac{\dot{\phi}\bar{c}}{V}\right)\left(\frac{2}{3} - \frac{1}{4}\frac{x_o}{\bar{c}}\right).$$

Therefore

$$-\frac{1}{2}\frac{\partial C_L}{\partial(\dot{\phi}V/\bar{c})} = -\pi A\left(\frac{2}{3} - \frac{1}{4}\frac{x_o}{\bar{c}}\right)$$

in the notation of Mangler and Garner, and becomes

$$z_{\dot{\phi}} = -(\pi A/4)(3-2h) \qquad \text{.....(32)}$$

in the notation of this report.

Similarly the pitching moment coefficient about the point $x=x_o$ is

$$C_m = \int_o^{2\bar{c}} \frac{l(x).(x-x_o)dx}{\frac{1}{2}\rho V^2 S\bar{c}}$$

$$= -2\pi A\left(\frac{\dot{\phi}\bar{c}}{V}\right)\left[1 - \frac{x_o}{\bar{c}} + \frac{1}{4}\left(\frac{x_o}{\bar{c}}\right)^2\right].$$

Therefore

$$\frac{1}{2}.\frac{\partial C_m}{\partial(\dot{\phi}\bar{c}/V)} = -\pi A\left[1 - \frac{x_o}{\bar{c}} + \frac{1}{4}\left(\frac{x_o}{\bar{c}}\right)^2\right]$$

or

$$m_{\dot{\phi}} = -\tfrac{1}{2}\pi A(h-1)^2 \qquad \text{.....(33)}$$

in the present notation, so that $m_{\dot{\phi}}$ has a minimum magnitude

of zero for the reference axis at the trailing edge, i.e. $x_o = 2\bar{c}$ or $h = 1.0$.

Garner, on the basis of the same theory, shows that for a taper ratio $\lambda = 1/7$

$$-\frac{1}{2}\frac{\partial C_L}{\partial(\dot{\phi}\bar{c}/V)} = -\pi A\left(\frac{5}{8} - \frac{1}{4}\frac{x_o}{\bar{c}}\right)$$

$$-\frac{1}{2}\frac{\partial C_m}{\partial(\dot{\phi}\bar{c}/V)} = -\pi A\left[\frac{49}{64} - \frac{7}{8}\frac{x_o}{\bar{c}} + \frac{1}{4}\left(\frac{x_o}{\bar{c}}\right)^2\right]$$

where $x_o/\bar{c}$ for the tapered delta wing is given by

$$\frac{x_o}{\bar{c}} = \frac{4}{3}\frac{h(1+\lambda+\lambda^2)}{(1+\lambda)^2} + \frac{2}{3}\frac{(1-\lambda)(1+2\lambda)}{(1+\lambda)^2}$$

$$= (4/3)(h+\tfrac{1}{2}) \quad \text{for} \quad \lambda = 0$$

$$= 1.190h + 0.560 \quad \text{for} \quad \lambda = 1/7.$$

Hence, for $\lambda = 1/7$,

$$z_{\dot{\phi}} = -\pi A\,(0.728 - 0.446h) \qquad \ldots\ldots\ldots\ldots(34)$$

in the notation of this report. It will be seen that the right hand side of equation (34) is very similar to that of (32) indicating that the effect of taper is roughly the same as that of a shift of pitching axis.

Similarly for $\lambda = 1/7$

$$m_{\dot{\phi}} = -0.4\,\pi A(h-1)^2 \qquad \ldots\ldots\ldots\ldots(35)$$

in the present notation.

This theory (Fig. 13) shows poor agreement with the theory of Multhopp-Garner or Lehrian even for an aspect ratio as low as 0.5 (see Figs. 14 and 15).

Lehrian uses the modified vortex lattice method due to W.P. Jones. Her calculations show good agreement in incompressible flow with the Multhopp-Garner method for the practical C.G. range of $0.4 < x_o/c_o < 0.6$. The Multhopp-Garner method extends Multhopp's subsonic lifting surface theory for steady flow to harmonic pitching oscillations of low frequency. The

local lift and pitching moments at a number of chordwise sections are determined from a set of linear equations satisfying the downwash conditions at two points of each section. By neglecting terms of second order in frequency (the theory holds for $\omega/(1-M_1^2) \ll 1$, and is therefore invalid near $M_1 = 1.0$), the oscillatory problem is related to a corresponding steady one with changed boundary conditions.

The theory provides what appears to be a reliable prediction of the effects of compressibility up to a Mach number of about 0.9 and indicates large increases in damping in pitch within this range for low aspect ratios. It leads to equations of the form, for $M_1 = 0$:

$$\frac{2}{3}\, z_{\dot{\phi}} = -\frac{1}{2}\frac{\partial C_L}{\partial(\dot{\phi}\bar{c}/V)} = -\frac{1}{2}\left\{C_{L2} + C_{L3} - (x_o/\bar{c})C_{L1}\right\}$$

$$\frac{8}{9}\, m_{\dot{\phi}} = +\frac{1}{2}\frac{\partial C_m}{\partial(\dot{\phi}\bar{c}/V)} = \frac{1}{2}\left\{C_{m2} + C_{m3} + (x_o/\bar{c})\left[-C_{m1} + C_{L2} + C_{L3}\right] - (x_o/\bar{c})^2 C_{L1}\right\}$$

$$\frac{2}{3}\, z_q = -\frac{1}{2}\frac{\partial C_L}{\partial(q\bar{c}/V)} = -\frac{1}{2}\left\{C_{L2} - (x_o/\bar{c})\, C_{L1}\right\}$$

$$\frac{8}{9}\, m_q = +\frac{1}{2}\frac{\partial C_m}{\partial(q\bar{c}/V)} = \frac{1}{2}\left\{C_{m2} + (x_o/\bar{c})(C_{m1} + C_{m2}) - (x_o/\bar{c})^2\, C_{L1}\right\},$$

where C_m is measured about the pitching axis at x_o, and C_{L1}, C_{L2}, C_{L3}, C_{m1}, C_{m2}, C_{m3} are coefficients depending on the geometry of the delta planform.

Similarly, for compressible flow,

$$\frac{2}{3}\, z_{\dot{\phi}} = -\frac{1}{2}\left\{\left[(1-\beta^2)\, I^{*}_{m1} + (2\beta^2-1)I_{L2} + I_{L3}\right]/\beta^3 - (x_o/\bar{c})I_{L1}/\beta\right\}$$

$$\frac{8}{9}\, m_{\dot{\phi}} = \frac{1}{2}\left\{\left[(1-\beta^2)I^{*}_{m} + (2\beta^2-1)I_{m2} + I_{m3}\right]/\beta^3 + (x_o/\bar{c})\left[I^{*}_{L} + (2\beta^2-1)\, I_{L2} + I_{L3}\right]/\beta^3 - (x_o/\bar{c})^2 I_{L1}/\beta\right\}$$

$$\frac{2}{3}\, z_q = -\frac{1}{2}\left[I_{L2} - (x_o/\bar{c})I_{L1}\right]/\beta$$

$$\frac{8}{9}\, m_q = \frac{1}{2}\left[I_{m2} + (x_o/\bar{c})(I^{*}_{L1} + I_{L2}) - (x_o/\bar{c})^2\, I_{L1}\right]/\beta,$$

where $\beta = \sqrt{1-M_1^2}$, and where I_{L1}, I_{L2}, I_{L3}, I^{*}_{L}, I_{m1}, I_{m2}, I_{m3}, I^{*}_{m} are coefficients depending on the equivalent wing in incompressible

flow (i.e. one with span reduced in the ratio $\beta : 1$).

The theories of Mangler,[12] Ribner and Malvestuto[15] are identical and limited to frequencies where $\bar{\omega}/(M_1^2-1) \ll 1$ for subsonic leading edges and supersonic Mach numbers. In the present notation they lead to the simple relations

$$z_q = -\frac{\pi A}{4E}(3H-2h-1)\, z_{\dot{\phi}} \qquad \text{.....(36)}$$

$$z_{\dot{w}} = -\frac{\pi A}{4E}\left[1 - \frac{3M_1^2(1-H)}{M_1^2-1}\right] z_{\dot{\phi}}$$

$$z_w = -\pi A/(4E)$$

$$m_w = z_w(\tfrac{1}{2}-h)$$

$$m_q = -\frac{\pi A}{4E}(2h^2-3hH+\frac{15}{8}H+\tfrac{1}{2})\, m_{\dot{\phi}}$$

$$m_{\dot{w}} = z_{\dot{w}}(\frac{5}{8}-h)\, m_{\dot{\phi}}$$

where $H = EG$

E = complete elliptic integral of second kind with modulus $k = \int_0^{\pi/2}(1-k^2\sin^2 x)^{\frac{1}{2}}\,dx$

$k^2 = 1 - \cot^2\mu \cot^2\Lambda$

$G = k^2 / \{(2k^2-1)E + (1-k^2)F\}$

F = complete elliptic integral of the first kind with modulus $k = \int_0^{\pi/2}(1-k^2\sin^2 x)^{-\frac{1}{2}}\,dx$

H and $1/E$ as functions of $\mu \cot\Lambda$ are shown in Fig.18.

The results indicate that the 45° delta has negative damping for the specified practical C.G. range of $0.4 < x_o/c_o < 0.6$ at $M_1 = 1.2$.

Ribner in Ref. 16, uses the assumptions of slender wing theory. The resulting stability derivatives within these assumptions apply at both subsonic and supersonic speeds.

The theory leads to the following formulae

$$
\begin{aligned}
z_w &= -\pi A/2 \\
z_{\dot{w}} &= -\pi A/4 \qquad & z_{\dot{\alpha}} &= -(\pi A/4)(3-2h) \\
z_q &= -(\pi A/2)(1-h) \\
m_w &= z_w(\tfrac{1}{2}-h) \\
m_{\dot{w}} &= z_{\dot{w}}(5/8-h) \qquad & m_{\dot{\alpha}} &= -(\pi A/2)(h-1)^2 \\
m_q &= -(\pi A/4)(2h^2-3h+11/8)
\end{aligned}
\qquad \ldots\ldots\ldots(37)
$$

We may note that, not unexpectedly, the theories of Mangler, Ribner and Malvestuto reduce to the above simple relations when we set $H = E = 1$, i.e. when $M_1 = 1.0$, and are identical with the results of the Low Aspect Ratio theory of Garrick. This theory, in effect, gives the slope of the $m_{\dot{\alpha}}$, $z_{\dot{\alpha}}$ curves for $A \to 0$, as shown in Figs. 14 to 17, but as can be gathered from those figures the theory has little reliability for any but very small values of aspect ratio.

Mangler has in Ref. 13 developed a theory restricted to low frequencies and incidences but it is claimed to be valid at $M = 1.0$. This theory indicates the important parameters influencing the damping through the transonic range and demonstrates the general trends. This theory leads to the following relations:

a) 'Steady' derivatives $(\bar{\omega} \to 0)$

$$
\begin{aligned}
z_w &= -\tfrac{1}{2}\pi A \\
m_w &= z_w(\tfrac{1}{2}-h) \\
z_q &= -\tfrac{1}{2}\pi A(1-h) \\
m_q &= -(\pi A/4)(2-h^2-3h+11/8)
\end{aligned}
\qquad \ldots\ldots\ldots(38)
$$

which are identical to the formulae given by Low Aspect Ratio theory of Garrick and Ribner.

b) 'Frequency Dependent' derivatives $(\bar{\omega} > 0)$

$$
\begin{aligned}
z_{\dot{w}} &= -(\pi A/4)k(\bar{\omega}) \\
z_{\dot{\alpha}} &= -(\pi A/4)(3-2h) + k'(\bar{\omega})
\end{aligned}
$$

$$m_{\dot{w}} = z_{\dot{w}}(5/8 - h) - (9/64)\pi \cot^3\Lambda$$

$$m_{\dot{\phi}} = -\tfrac{1}{2}\pi A(h-1)^2 + (5/8-h)k'(\bar{\omega}) - (9/64)\pi \cot^3\Lambda \quad \ldots\ldots\ldots\ldots(39)$$

which include the additional factors dependent on frequency:

$$k(\bar{\omega}) = 1 - \tfrac{1}{2}\cot^2\Lambda \left[4.959 - 3\ln(\bar{\omega}\cot^2\Lambda)\right]$$

$$k'(\bar{\omega}) = \tfrac{1}{2}\pi\cot^3\Lambda \left[4.959 - 3\ln(\bar{\omega}\cot^2\Lambda)\right] \quad \ldots\ldots(40)$$

These relations are identical with those given by the Low Aspect Ratio theory of Garrick and Ribner if we set $k(\bar{\omega}) = 1$ and $k'(\bar{\omega}) = 0$, i.e. set $3\ln(\bar{\omega}\cot^2\Lambda) = 4.959$ and neglect the term $(9/64)\pi\cot^3\Lambda$ which is small for low aspect ratios.

With the aid of the results of the various theories which are illustrated in Figs. 14 to 18 and in the light of the available experimental evidence the curves of Figs. 19 to 24 were prepared for the two delta plan forms considered. No great accuracy can be claimed for these curves, particularly in the transonic range, which can only at the best be regarded as plausible guides to the truth.

It should be noted however that the theories on which these curves are based assume that the frequency parameter $\bar{\omega}$ is small. In the examples chosen the frequency parameter for the short period oscillation has in fact a maximum value of 0.6 which cannot be regarded as small, and undoubtedly all the derivatives, both damping and stiffness, may be appreciably dependent on frequency for values of the frequency parameter of this order. In the absence of reliable experimental data, however, it was considered that there would be little to gain from an attempt to allow for these frequency effects in this analysis.

We can conclude from this brief review of the damping derivatives of the delta wing that

a) the moment-acceleration derivative $m_{\dot{w}}$ can be safely neglected at sub-critical speeds.

b) within the practical C.G. range, the values of the damping derivatives in incompressible flow are relatively

insensitive to changes of aspect ratio for aspect ratios less than 4.

c) there is a positive contribution to damping from the derivatives z_q and m_q at all Mach numbers. Thus the possibility of overall instability (i.e. $z_{\dot{\phi}}$ or $m_{\dot{\phi}} > 0$) at transonic speeds arises from the increases in z_w and m_w. These derivatives can be decreased by a forward shift of C.G. but the shift requires to be impracticably large to achieve a major improvement.

d) The 'stiffness' of the short period oscillation depends largely on the variation of m_w, and this derivative increases with Mach number to a maximum in the transonic speed range. This increase implies an increase in frequency, which in turn implies that instability at transonic speeds is more serious because the amplitude of the oscillatory acceleration will grow all the more rapidly and dangerously. Our concern is, therefore, with the possibility of short period oscillations with negative damping.

8. Formulation of a Standard of Minimum Level of Damping for a Delta Planform

From equations (7) and (8), we have,

$$\text{cycles to half amplitude} \approx \frac{0.2206\sqrt{(m_q z_w - \mu_1 m_w)/i_B}}{-z_w - m_{\dot{\phi}} / i_B} .$$

This relation is increasingly more accurate at high μ_1, i.e. at high altitude where the damping will be most critical.

If we now specify that the minimum allowable number of cycles to half amplitude shall be one, the maximum allowable value of $m_{\dot{\phi}}$ is

$$m_{\dot{\phi}_{max}} \approx -z_w i_B - 0.2206\sqrt{i_B(m_q z_w - \mu_1 m_w)} \quad \ldots\ldots(41)$$

We may compare this value with the actual value of the damping derivative, the difference $\Delta m_{\dot{\phi}} = m_{\dot{\phi}_{max}} - m_{\dot{\phi}}$ then gives a measure of the comparative damping qualities of the delta planforms

of varying sweep.

The results of such an analysis are shown in Figs. 25 and 26, where the effect of varying sweep, Mach number, C.G. position and relative density are illustrated.

It will be seen that there are diminishing returns in damping for increased sweep. In fact, little advantage is to be gained for sweep angles greater than about 60°. Forward movement of the C.G. improves the damping but this is counterbalanced by the increased stiffness of the oscillation for $\Lambda > 60^\circ$. A 45° tailless delta appears to have inadequate damping in the transonic range of Mach numbers.

These conclusions are of course, subject to some measure of doubt insofar as the basic curves for the damping derivatives, Figs. 19 to 22, are little more than plausible guesses. Nevertheless the trends of the results are almost certainly significant.

9. The Coefficients of the Stability Quartic and some deductions

We are now in the position to estimate the coefficients of the stability quartic, from which we can deduce the frequency and damping of the short and long period contributions to the oscillatory motion of the aircraft. The values of the coefficients are shown plotted in Figs. 27 to 31 as functions of Mach number for relative density, $\mu_1 = 50$.

Figs. 28 and 29 show that, except very near $M_1 = 1.0$, a good approximation can be made to the short period damping coefficient B and stiffness coefficient C by neglecting x_u, $z_{\dot{w}}/\mu_1$, and z_q/μ_1. The quantity $\sqrt{m_w/\mu_1 i_B}$ is shown in Fig.32 to be a good first approximation to the short period frequency parameter to $= 2\pi f\bar{c}/V$, where f is the frequency for the C.G. position considered.

Figure 33 shows the cycles to damp to half amplitude and demonstrates the need of a tailplane for the parameters considered in the case of the 45° delta to correct the serious instability in the range $0.97 < M_1 < 1.5$. The figure also suggests

that μ_1 should not exceed 200 for the tailless 60° delta to remain adequately damped.

It is well known that the coefficients E and C in the stability quartic are related to the static and manoeuvre margins respectively. Thus, it can be readily shown that

$$E = -2\frac{\mu_1}{i_B} C_L^2 \frac{\partial C_L}{\partial a}\left(\frac{dC_m}{dC_L}\right)_{C_L M_1^2=\text{const.}} = 2\frac{\mu_1}{i_B} C_L^2 \frac{\partial C_L}{\partial a} K_n \quad \ldots(42)$$

where K_n is the static margin (stick fixed) $= -(dC_m/dC_L)_{C_L M_1^2=\text{const.}}$, and with some approximation

$$C = -\frac{\mu_1}{i_B}\frac{\partial C_L}{\partial a} H_m$$

where H_m is the manoeuvre margin (stick fixed).
K_n and H_m are shown plotted in Figs. 34 and 35 and can be compared with E and C in Figs. 31 and 29 respectively.

10. Possibilities of Improving the Damping Derivative m_ϕ

Improvements to the damping derivative m_ϕ can be made by the addition of a forebody, foreplane, or tailplane or by cropping the wing tips.

Applying Munk's Slender Body Theory, an estimate of the additional damping due to fuselage is,

$$\Delta m_\phi \simeq -2B_v (l-x)^2/(S\bar{c}^2),$$

where B_v = body base cross sectional area $= \pi a^2/4$,

l = body length measured forward from wing apex,

x = distance from C.G. to nose.

Therefore

$$\Delta m_\phi \simeq -\tfrac{1}{2}\pi d^2 (l-x)^2/(S\bar{c}^2) \quad \ldots\ldots\ldots\ldots(43)$$

For a representative case, where $S = 1000$ ft.^{2}, $\bar{c} = 30$ ft., $l = 20$ ft., $x = 35$ ft., $d = 10$ ft., we obtain $\Delta m_\phi = -0.05$,

a small, but significant value at transonic speeds.

Cropping the tips, and thus reducing the aspect ratio, is not quite so effective as reduction of aspect ratio by increased sweepback. The change in m_{ϕ} due to cropping is closely equivalent to that due to a shift of axis according to the geometrical relation

$$h = \frac{x_o}{\bar{c}} - \frac{1 + \lambda - 2\lambda^2}{2(1+\lambda+\lambda^2)} \qquad \text{(See section 7).}$$

For example, for a C.G. at $h = 0.25$ with a 'true' delta, the equivalent axis for a taper of $1/7$ is $h = 0.37$ (i.e. $x_o/c_o = 0.70$).

From Figure 17 it is noted that for a 45° delta this will give a substantial increase in $-m_{\phi}$ at $M_1 = 1.2$, but this is not the case for the 60° delta. From Figure 15 a slight decrease in m_{ϕ} can be expected at subsonic speeds therefore the tip cropping will not produce similar gains in all cases, but it appears to be very effective with the 45° delta at transonic speeds as shown in Fig. 36.

11. Some simple response calculations

As an example of the response of the 45° tailless delta we will consider the simple case of two degrees of freedom, i.e. we will neglect disturbances in forward velocity, the elevon will be assumed applied instantaneously but the additional lift due to control deflection will be neglected.

The equations of motion simplify to:

$$-\left(\frac{z_{\dot{w}}}{\mu_1} - 1\right)\frac{d^2\hat{w}}{d\hat{t}^2} + \frac{d\hat{w}}{d\hat{t}}\left[-\frac{m_{\dot{w}}}{i_B}\left(\frac{z_q}{\mu_1} + 1\right) - z_w + \frac{m_q}{i_B}\left(\frac{z_{\dot{w}}}{i_B} - 1\right)\right]$$
$$-\left[\frac{\mu_1}{i_B} m_w \left(\frac{z_q}{\mu_1} + 1\right) - \frac{m_q}{i_B} z_w\right] w = m_o \qquad \text{.....(44)}$$

the solution of which is:

$$\frac{\hat{w}}{m_o} = \frac{1}{k}\left[1 - \frac{\sqrt{k}}{\sqrt{k-(\frac{1}{2}b)^2}} \exp\left(-\tfrac{1}{2}b\hat{t}\right)\sin\left\{\sqrt{k-(\tfrac{1}{2}b)^2} + \tan^{-1}\frac{\sqrt{k-(\frac{1}{2}b)^2}}{\frac{1}{2}b}\right\}\right]$$

where

$$b = \frac{m_{\dot{w}}}{i_B}\frac{(z_q/\mu_1+1)}{(z_{\dot{w}}/\mu_1-1)} + \frac{z_w}{(z_{\dot{w}}/\mu_1-1)} - \frac{m_q}{i_B} \approx B \quad \ldots\ldots(45)$$

and

$$k = \frac{\mu_1}{i_B} m_w \frac{(z_q/\mu_1+1)}{(z_{\dot{w}}/\mu_1-1)} - \frac{m_q}{i_B}\frac{z_w}{(z_{\dot{w}}/\mu_1-1)} \approx C .$$

The effect of Mach number on this response is shown in Figure 37. The increase in damping and frequency with Mach number at subcritical speeds will be apparent, as will be the dangerous instability at $M_1 = 1.0$ coupled with high frequency, and the poor damping and high frequency at supersonic speeds is also evident.

A second example of response illustrating the effect of neglecting the damping in lift derivatives z_q and $z_{\dot{w}}$ is shown in Figure 38.

REFERENCES

1. Durand, W.F. — Aerodynamic theory, Vol. V. Berlin, Springer, 1934.

2. Duncan, W.J. — The principles of control and stability of aircraft. Cambridge, 1952.

3. Kell, C. — Comparative drag measurements on related planforms of 60° sweep back at transonic speeds using the ground launched rocket boosted model technique. R.A.E. Tech. Memo. No. Aero. 145, 1950.

4. Poulter, Y. — Comparative drag tests on three related 45° delta wings using ground launched rocket boosted models. R.A.E. Tech. Memo. No. Aero. 117, 1950.

5. Ross, J.G., Hills, R., and Bock, R.C. — Wind tunnel tests on a 90° apex delta wing of variable aspect ratio. Parts I and II. A.R.C. Current Paper No. 83, 1952.

6. Robinson, A. — Lift and drag of a flat delta wing at supersonic speeds. R.A.E. Tech. Note No. Aero. 1791, 1946.

7. De Young, J. — Theoretical additional span loading characteristics of wings with arbitrary sweep, aspect ratio, and taper ratio. N.A.C.A., T.N. No. 1491.

8. Milliken, W.(Jr.) — Dynamic stability and control research. Anglo-American Conference, 1951.

9. Garner, H.C. — Multhopp's subsonic lifting surface theory of wings in slow pitching oscillations. A.R.C. Report No. 15,096, 1952.

10. Lehrian, D.E. — Aerodynamic coefficients for an oscillating delta wing. A.R.C. Report No. 14,156, 1951.

11. Lehrian, D.E. — Calculation of stability derivatives for oscillating wings. A.R.C. Report No. 15,695, 1953.

12. Mangler, K.W. — The short period longitudinal derivatives of a delta wing at supersonic speeds. R.A.E. Tech. Note No. Aero. 2099, 1945.

13. Mangler, K.W. — A method of calculating the short period longitudinal stability derivatives of a wing in linearized unsteady compressible flow. R.A.E. Tech. Rep. No. Aero. 2468, 1950.

14. Garrick, J.E. — Some research on high speed flutter. Anglo-American Conference, 1951.

15. Ribner, H.S., and Malvestuto, F.S.(Jr.) — Stability derivatives of triangular wings at supersonic speeds. N.A.C.A., T.R. No. 908, 1947.

16. Ribner, H.S. — The stability derivatives of low aspect ratio triangular wings at subsonic and supersonic speeds. N.A.C.A., T.N. No. 1423, 1947.

17. Stanton-Jones, R. — An empirical method for rapidly determining the loading distributions on swept-back wings. College of Aeronautics Rep. No. 32, 1950.

18. Neumark, S. — Dynamic longitudinal stability in level flight, including the effects of compressibility and variations of atmospheric characteristics with height. R.A.E. Tech. Rep. No. Aero. 2265, 1948.

19. Stanbrook — Analysis of theoretical and experimental data on the lift of wings with parallel tips at supersonic speeds. A.R.C. Rep. No. 14396 , F.M. 1629.

20. Bryant, L.W., and Gates, S.B. — Nomenclature for stability coefficients. Revised edition. A.R.C. Report No. 13,698, 1951.

21. Perkins, C.D., and Hage, R.E. — Airplane performance, stability, and control. John Wiley and Sons, New York, 1950.

APPENDIX

Definition of Derivatives

Factors to relate derivatives etc. as defined in this report to corresponding American and British derivatives and coefficients as defined in sources listed below.

Derivative or coefficient as defined in this report	Garrick, Garner, Mangler.	Ribner, Malvestuto.	Lehrian	Duncan	Perkins, Hage.
x_u	$2x_u$	-	-	$2x_u$	$-2C_D-M\left(\frac{\partial C_D}{\partial M}\right)_a$
x_w	$2x_w$	-	-	$2x_w$	$C_L - C_{Da}$
$x_{\dot{w}}$	-	-	-	-	-
x_q	-	-	-	$2\frac{l_t}{\bar{c}}x_q$	-
z_u	$2z_u$	-	-	$2z_u$	$-2C_L-M\left(\frac{\partial C_L}{\partial M}\right)_a$
z_w	$2z_w$	$-C_{La} - C_D$	$-2l_a-C_D$	$2z_w$	$-C_{La} - C_D$
$z_{\dot{w}}$	$\frac{3}{2}z_{\dot{w}}$	$\frac{1}{2}C_{L\dot{a}}$	$\frac{3}{2}l_{\dot{a}}$	-	-
z_q	$\frac{3}{2}z_q$	$-\frac{1}{2}C_{Lq}$	-	$2\frac{l_t}{\bar{c}}z_q$	-
m_u	$2m_u$	-	-	$2\frac{l_t}{\bar{c}}m_u$	C_{Mu}
m_w	$\frac{3}{2}m_w$	C_{Ma}	$\frac{3}{2}m_a$	$2\frac{l_t}{\bar{c}}m_w$	C_{Ma}
$m_{\dot{w}}$	$\frac{9}{8}m_{\dot{w}}$	$\frac{1}{2}C_{M\dot{a}}$	$\frac{9}{8}m_{\dot{a}}$	$2\frac{l_t^2}{\bar{c}^2}m_{\dot{w}}$	$\mu_{\bullet}C_{M_{d\alpha}}$
m_q	$\frac{9}{8}m_q$	$\frac{1}{2}C_{Mq}$	-	$2\frac{l_t^2}{\bar{c}^2}m_q$	$\mu_{\bullet}C_{M_{d\theta}}$
τ	2τ	2τ	-	2τ	2τ
$\hat{t}$	$2\hat{t}$	$2\hat{t}$	-	$2\hat{t}$	$2\hat{t}$
μ	$\frac{3}{2}\mu$	2μ	-	$2\frac{l_t}{\bar{c}}\mu_1$	2μ

Derivative or coefficient as defined in this report	Garrick, Garner, Mangler.	Ribner, Malvestuto.	Lehrian	Duncan	Perkins, Hage.
Standard Length	$\frac{4}{3}\bar{c}$	$\bar{\bar{c}}$	$\frac{4}{3}\bar{c}$	$\frac{\bar{\bar{c}}}{l_t} \cdot l_t$	$\bar{\bar{c}}$
i_B	$\frac{9}{16} i_B$	$\frac{I_y}{mc^{\bar{\bar{2}}}} = \frac{k_y^2}{\bar{\bar{c}}^2}$	-	$\frac{l_t^2}{\bar{\bar{c}}^2} i_B$	$\frac{\mu}{2} h$
ω	$\frac{4}{3}\omega$	-	-	$\frac{4}{3}\omega$	-
C_D	C_D	C_D	C_D	C_D	C_D
C_L	C_L	C_L	$2k_L$	C_L	C_L
C_M	$\frac{3}{4} C_M$	C_M	$\frac{3}{2} k_M$	$\frac{3}{4} C_M$	C_M

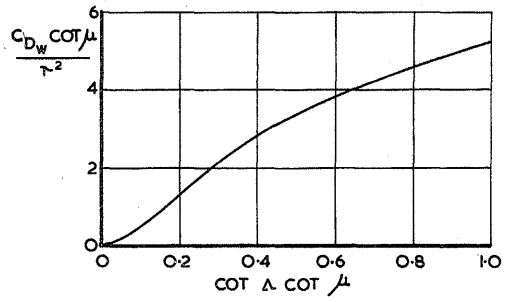

WAVE DRAG AT ZERO LIFT.

FIG. 1.

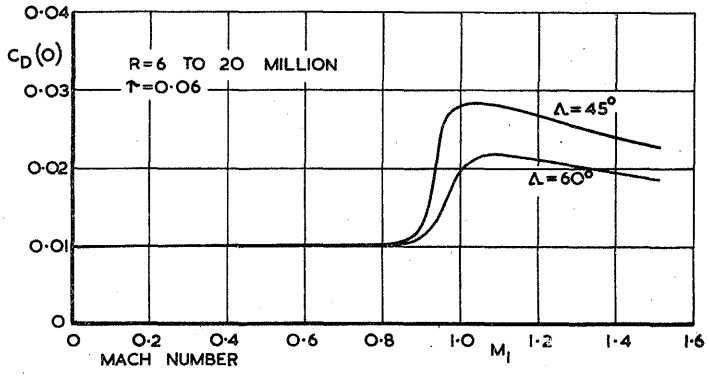

DRAG COEFFICIENT AT ZERO LIFT. DELTA PLANFORM.

FIG. 2.

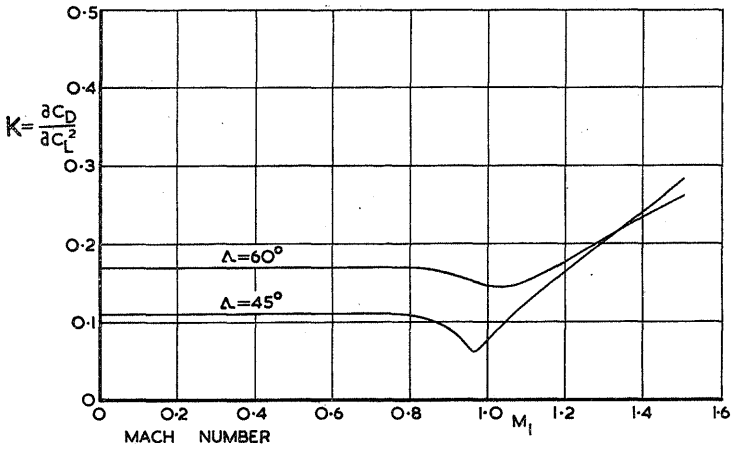

DRAG DUE TO LIFT. DELTA PLANFORM.

FIG. 3.

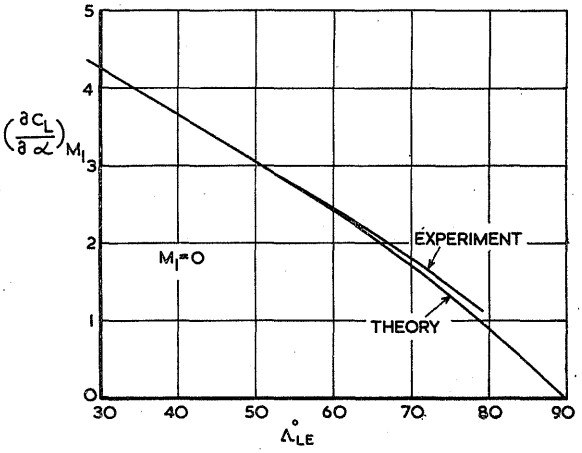

SLOPE OF LIFT CURVE FOP VARIOUS SWEEP ANGLES. INCOMPRESSIBLE FLOW.

FIG. 4.

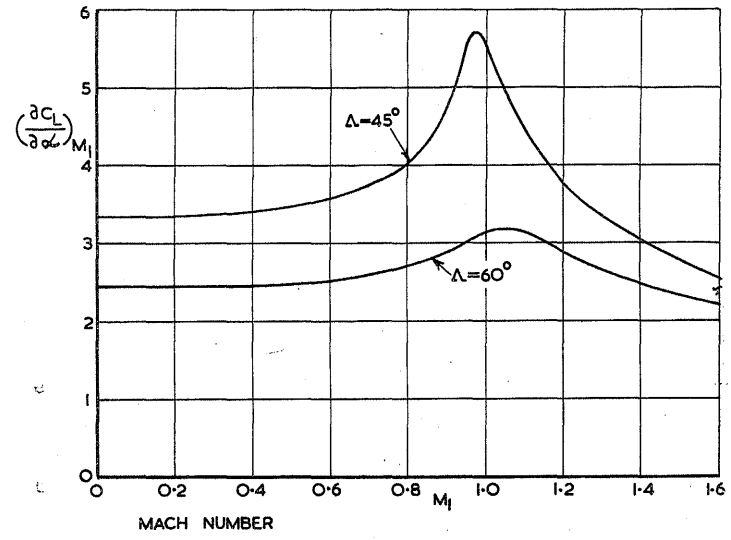

SLOPE OF THE LIFT CURVE. DELTA PLANFORM.

FIG. 5.

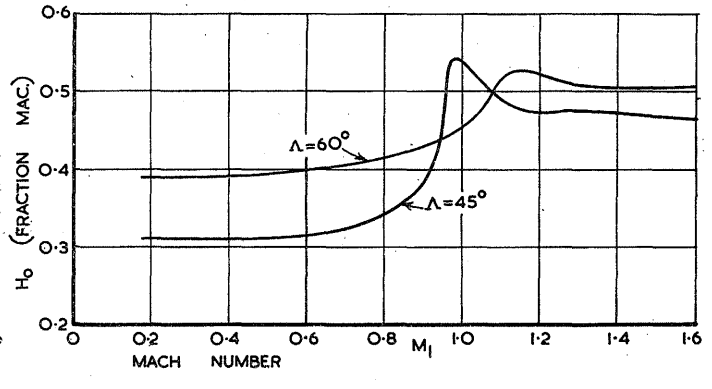

AERODYNAMIC CENTRE. DELTA PLANFORM.

FIG. 6.

FIGS. 7 TO 12.

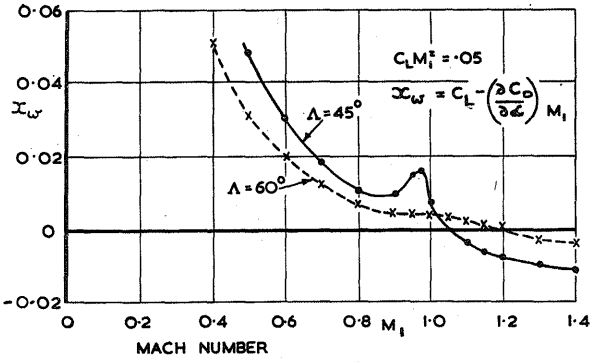

FORCE LINEAR VELOCITY DERIVATIVE x_ω
FIG. 7.

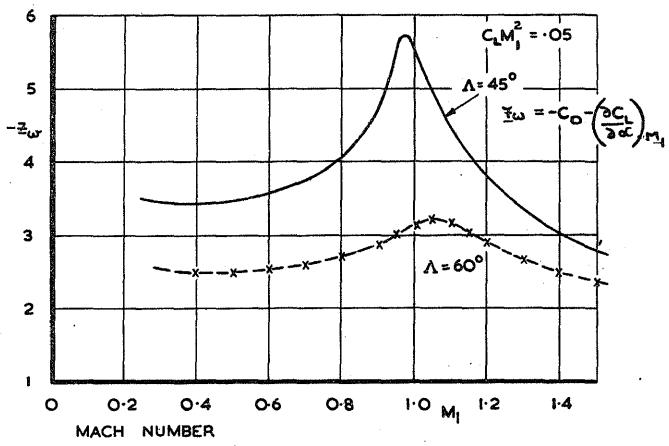

FORCE LINEAR VELOCITY DERIVATIVE Z_ω
FIG. 8.

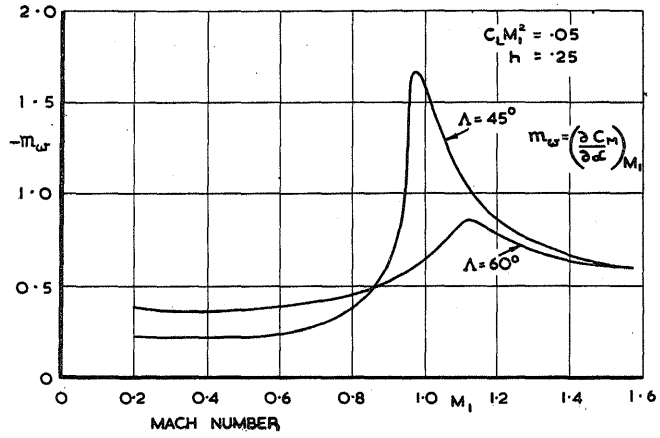

MOMENT LINEAR VELOCITY DERIVATIVE m_ω
FIG. 9.

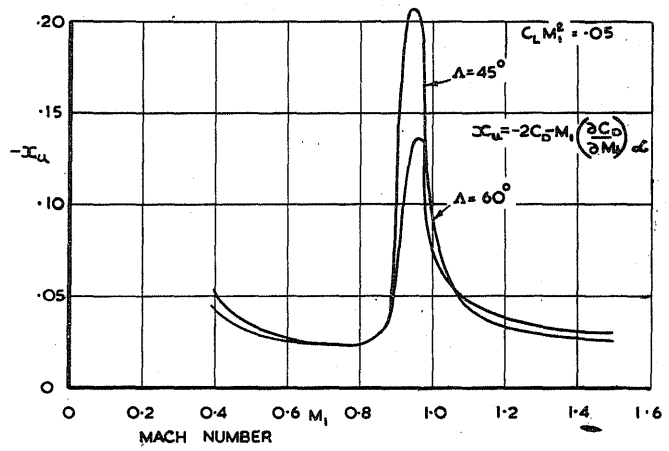

FORCE LINEAR VELOCITY DERIVATIVE x_u
FIG. 10.

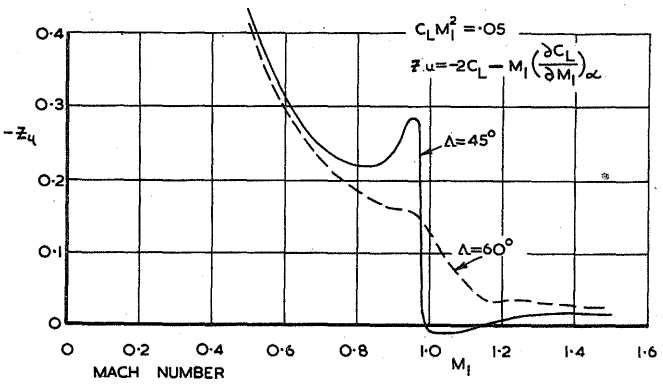

FORCE LINEAR VELOCITY DERIVATIVE Z_u
FIG. 11.

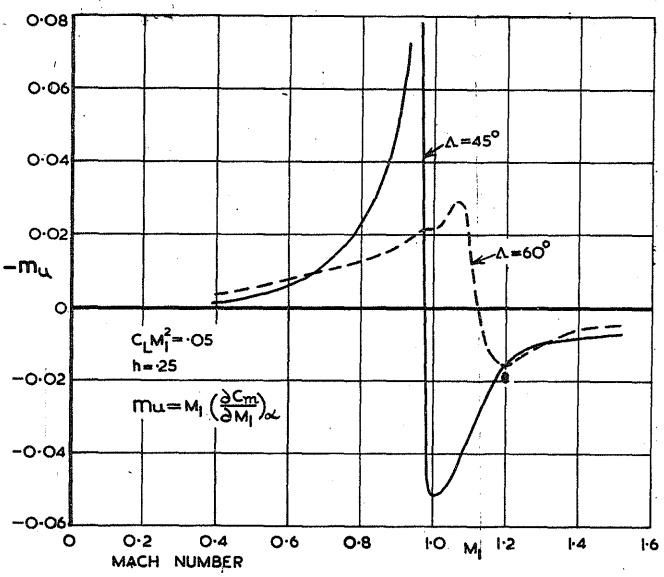

MOMENT LINEAR VELOCITY DERIVATIVE m_u
FIG. 12.

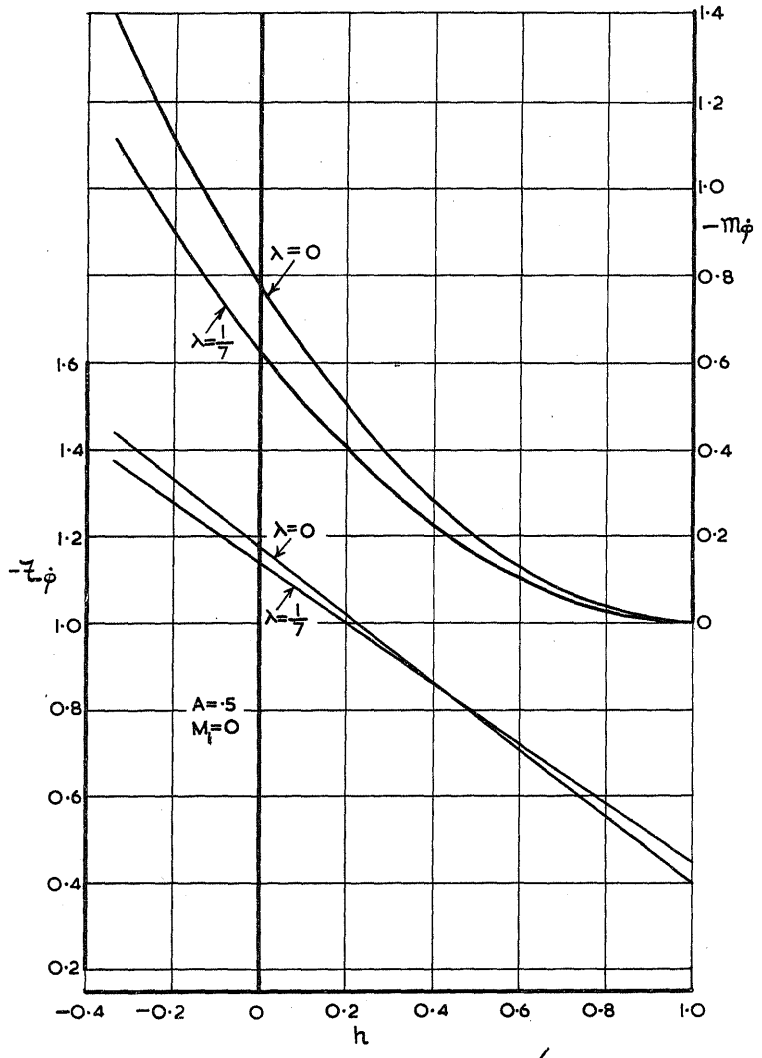

LOW ASPECT RATIO THEORY.
DELTA PLANFORM.
FIG. 13.

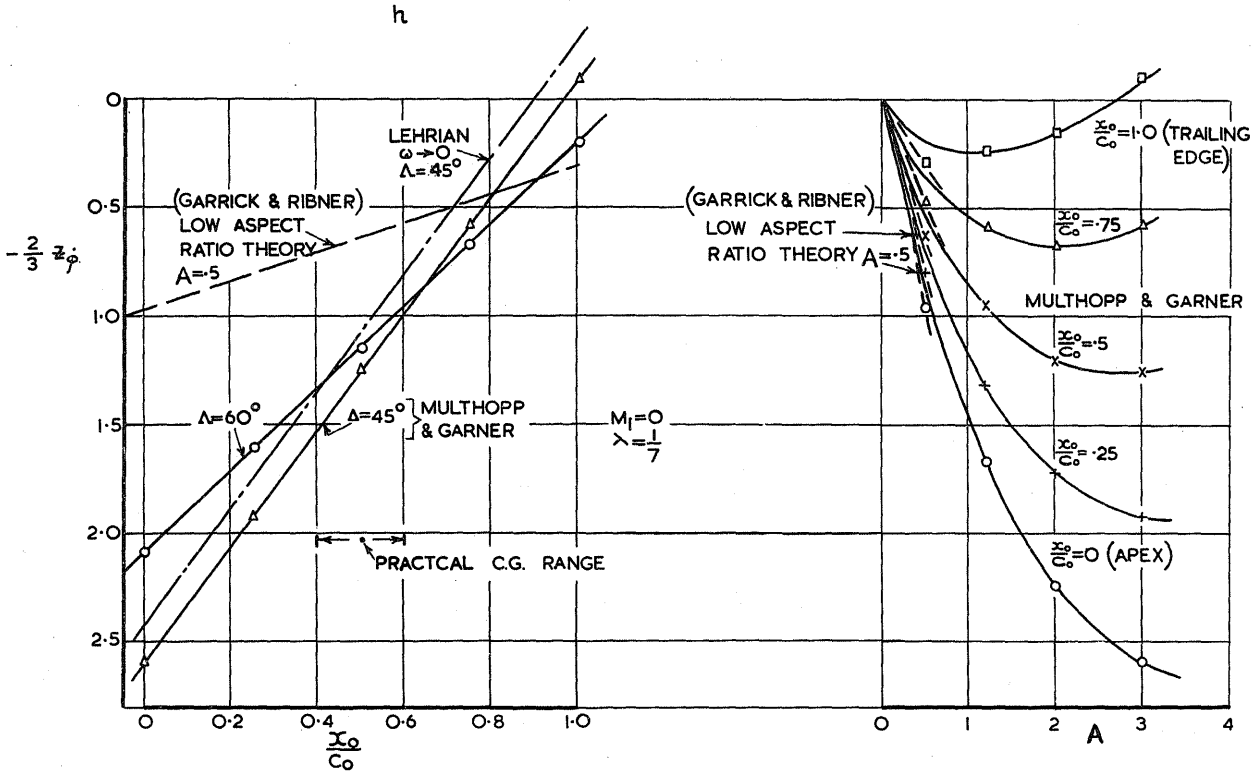

INCOMPRESSIBLE DAMPING IN PITCH. DELTA PLANFORM.
FIG. 14.

FIGS. 15 & 16.

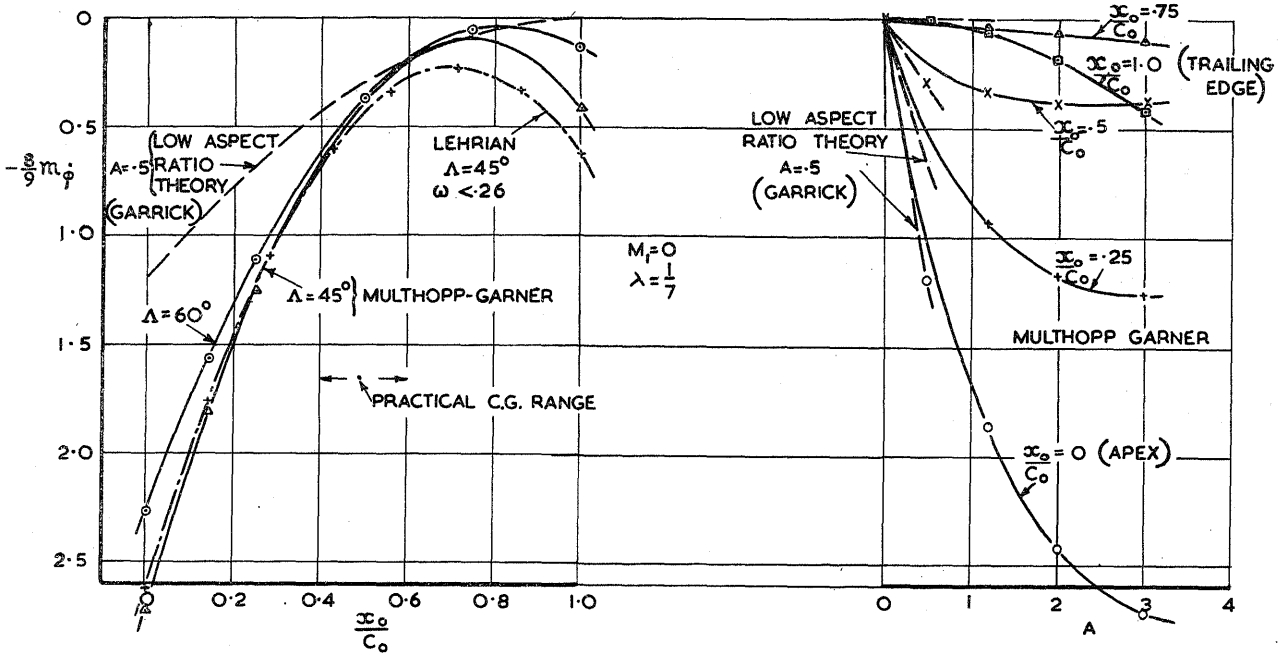

INCOMPRESSIBLE DAMPING IN PITCH DERIVATIVE. DELTA PLANFORM.

FIG. 15.

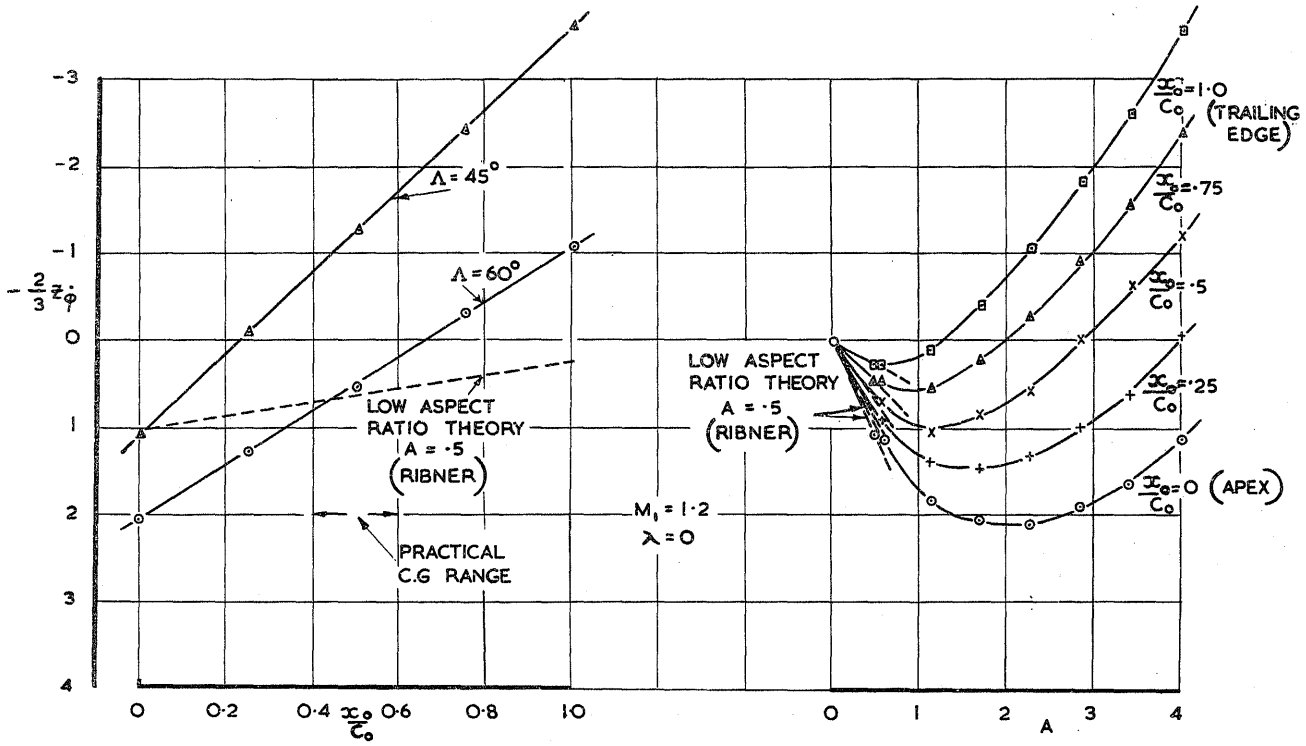

SUPERSONIC DAMPING IN PITCH. DELTA PLANFORM. (MANGLER RIBNER & MALVESTUTO.)

FIG. 16.

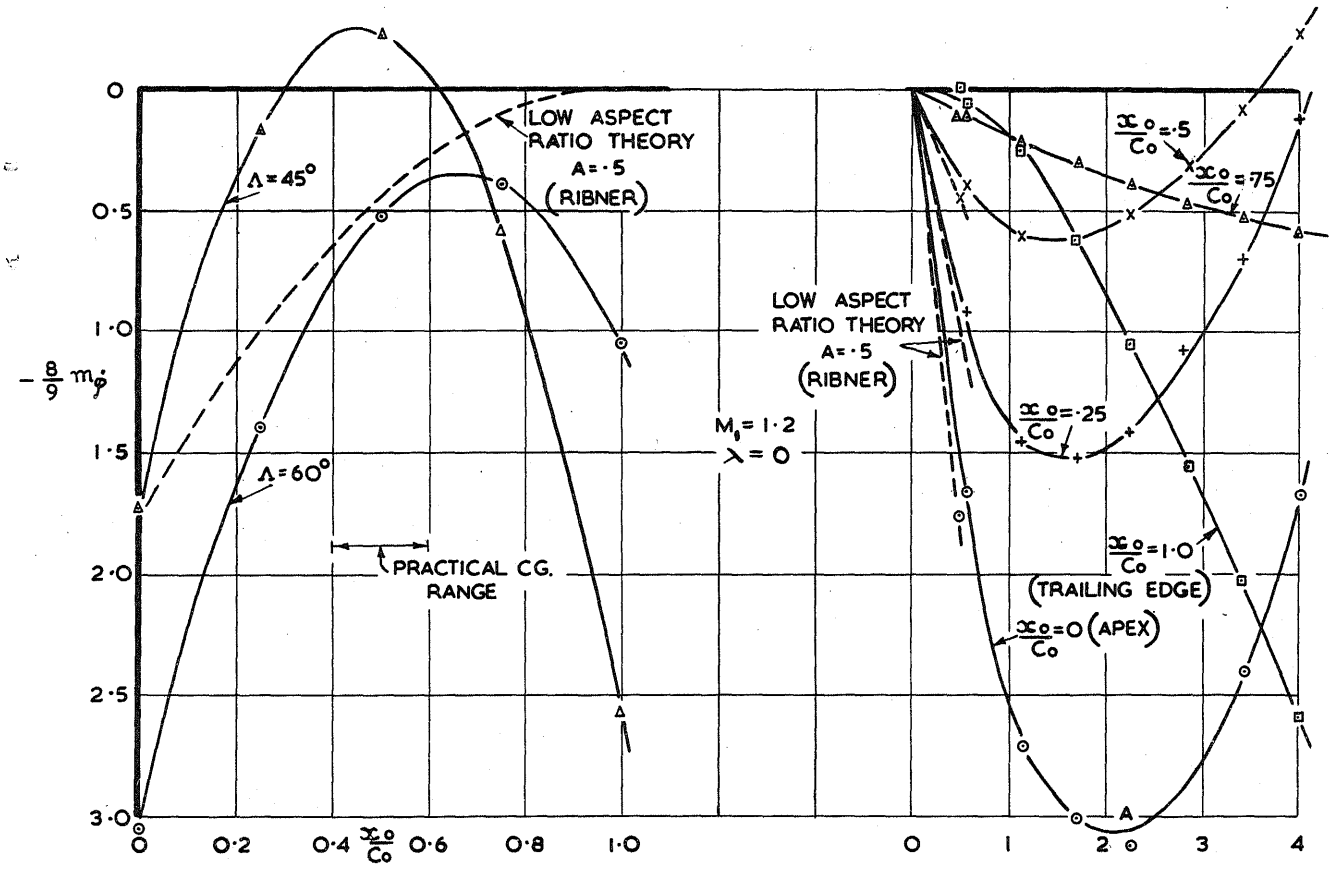

SUPERSONIC DAMPING IN PITCH DERIVATIVE. DELTA PLANFORM. MANGLER, RIBNER & MALVESTUTO.

FIG. 17.

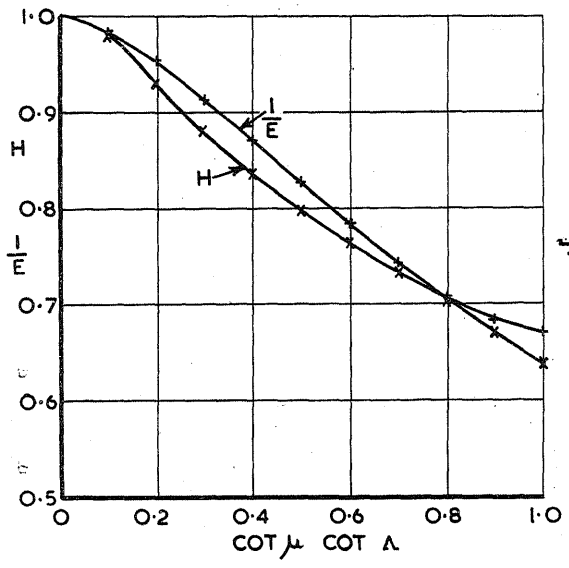

FUNCTIONS H, E REQUIRED IN THEORY OF MANGLER, RIBNER & MALVESTUTO

FIG. 18.

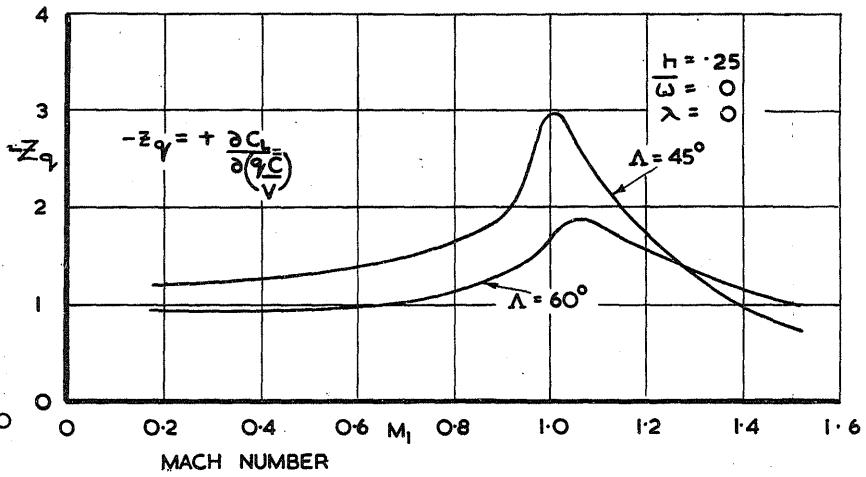

FORCE ANGULAR VELOCITY DERIVATIVE Z_q, DELTA PLANFORM.

FIG. 19.

FIGS. 20 TO 23.

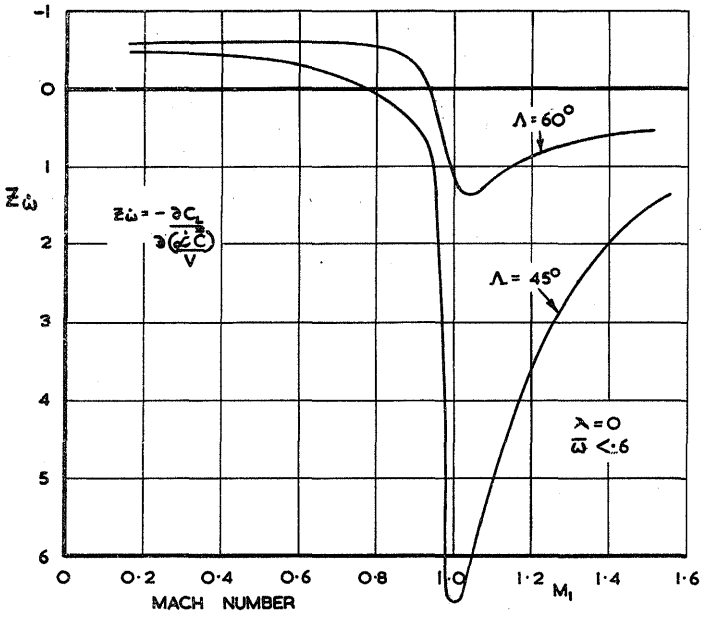

FORCE ACCELERATION DERIVATIVE $Z_{\dot{\omega}}$
DELTA PLANFORM.

FIG. 20.

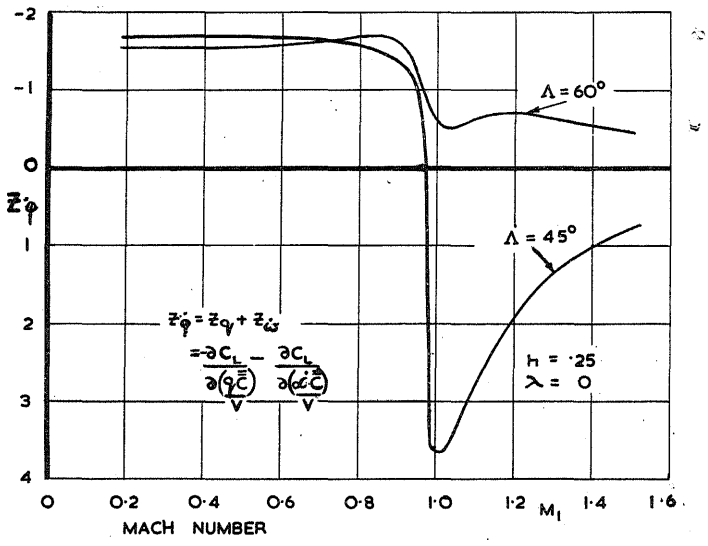

DAMPING IN PITCH DERIVATIVE $Z_{\dot{\phi}}$.
DELTA PLANFORM.

FIG. 21.

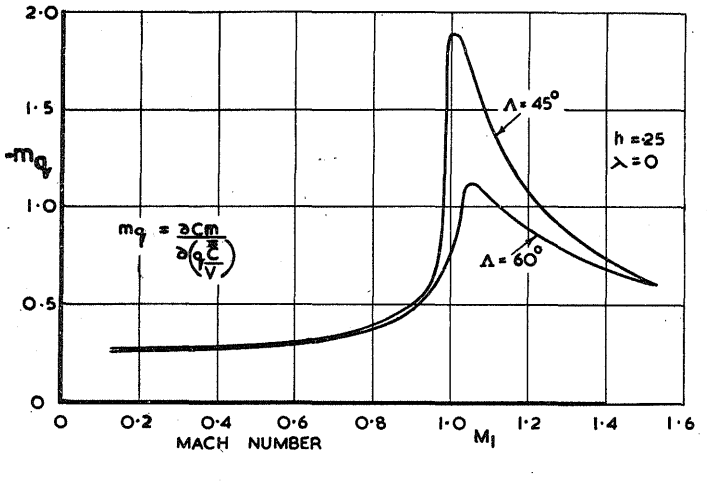

MOMENT ANGULAR VELOCITY DERIVATIVE m_q
DELTA PLANFORM

FIG. 22.

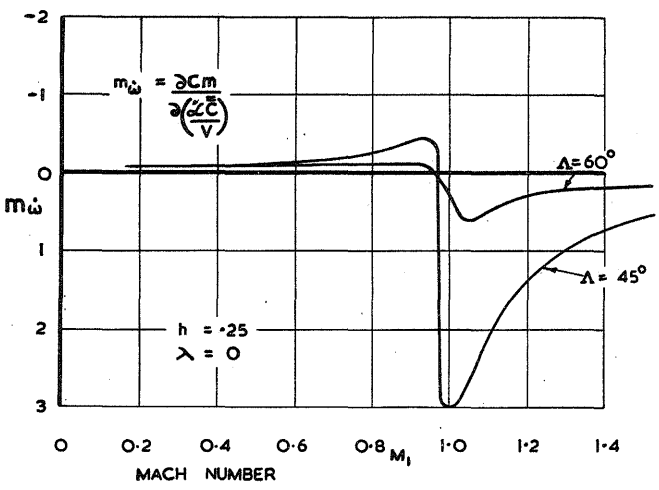

MOMENT ACCELERATION DERIVATIVE $m_{\dot{\omega}}$
DELTA PLANFORM

FIG. 23.

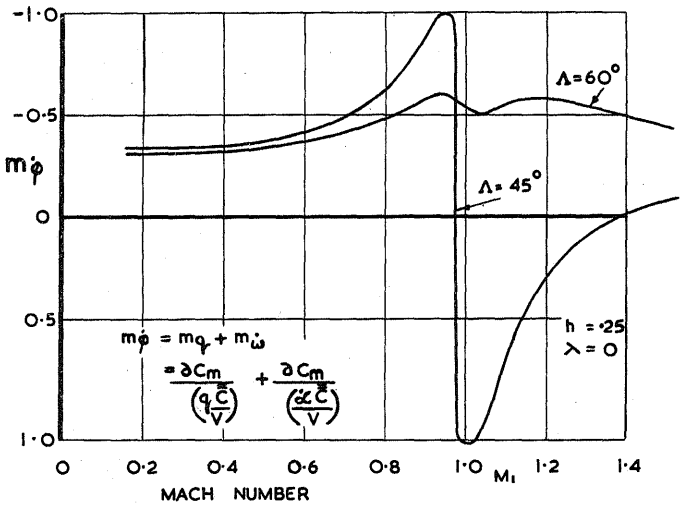

DAMPING IN PITCH DERIVATIVE $m_{\dot\phi}$.
DELTA PLANFORM.
FIG. 24.

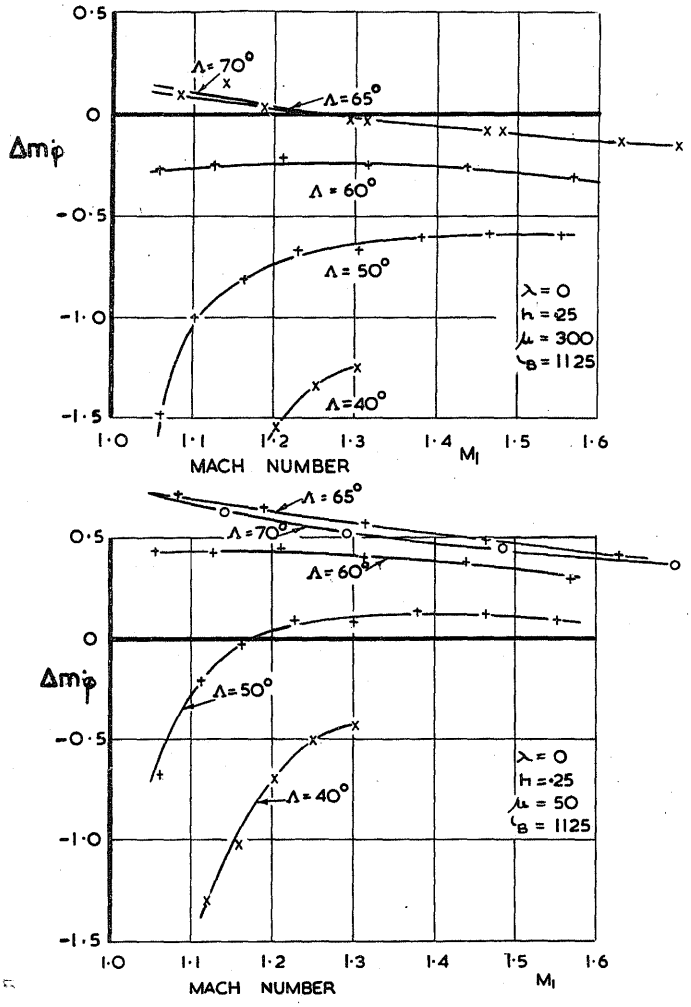

FIG. 25.

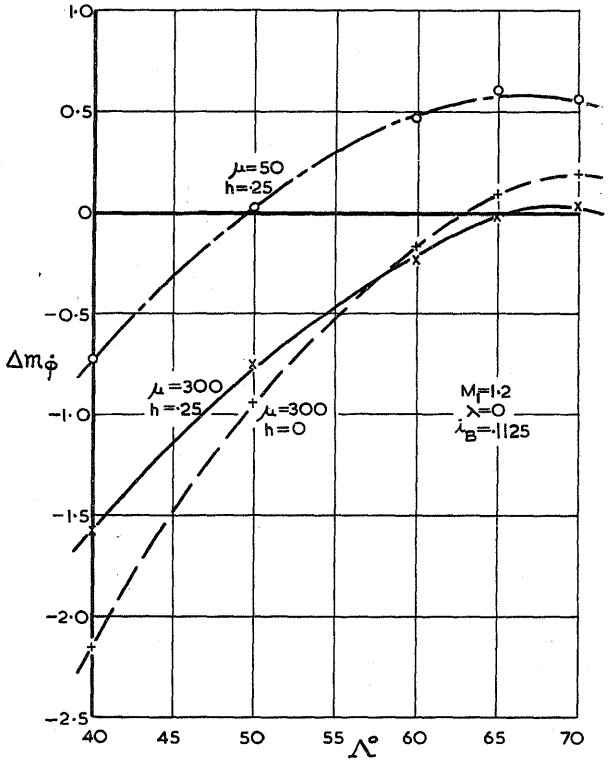

FIG. 26.

A MEASURE OF THE ABILITY OF THE DELTA PLANFORM TO DAMP THE SHORT PERIOD OSCILLATION TO HALF AMPLITUDE IN ONE CYCLE.

FIGS. 27 TO 32.

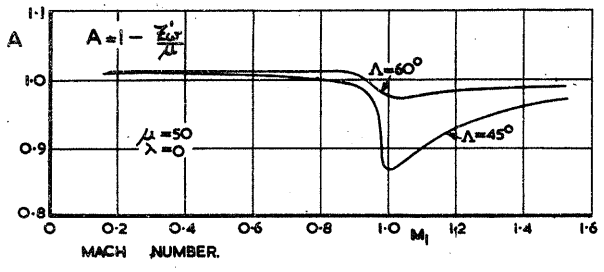

THE COEFFICIENT A OF THE STABILITY QUARTIC. DELTA PLANFORM.

FIG. 27.

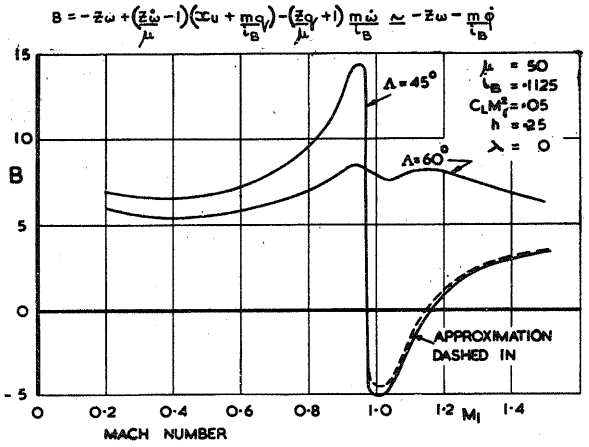

THE COEFFICIENT B OF THE STABILITY QUARTIC. DELTA PLANFORM.

FIG. 28.

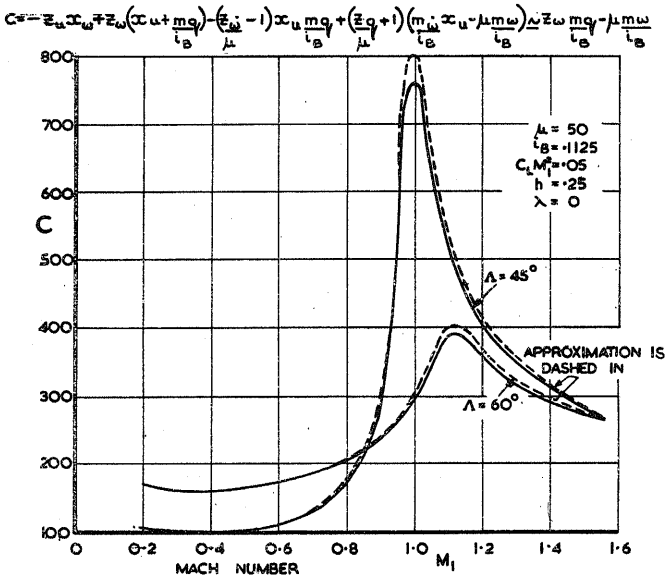

THE COEFFICIENT C OF THE STABILITY QUARTIC. DELTA PLANFORM.

FIG. 29.

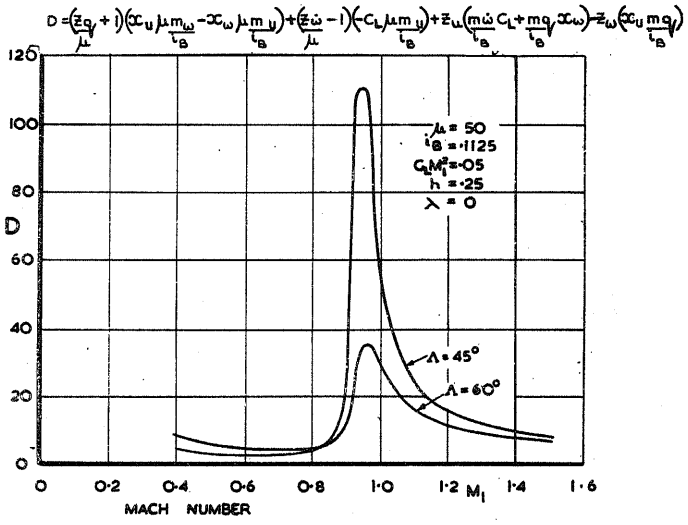

THE COEFFICIENT D OF THE STABILITY QUARTIC. DELTA PLANFORM.

FIG. 30.

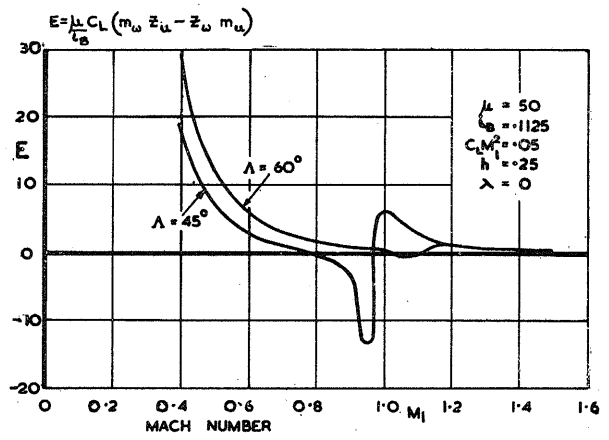

THE COEFFICIENT E OF THE STABILITY QUARTIC. DELTA PLANFORM.

FIG. 31.

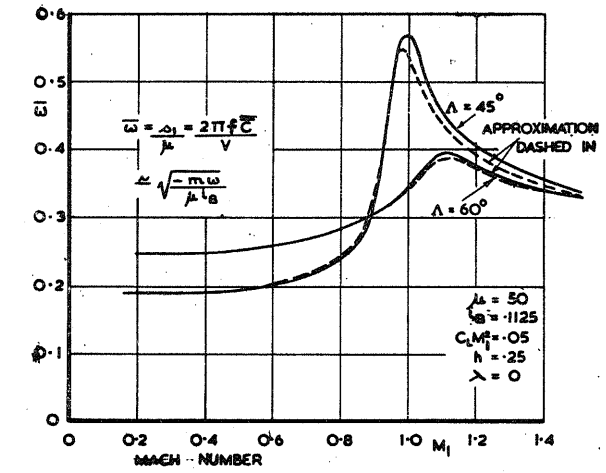

THE FREQUENCY PARAMETER $\bar{\omega}$ SHORT PERIOD OSCILLATION. DELTA PLANFORM.

FIG. 32.

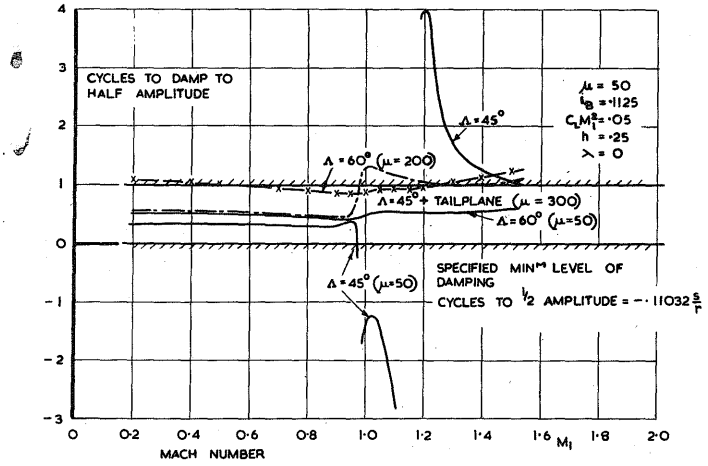

CYCLES TO DAMP TO HALF AMPLITUDE.

FIG. 33.

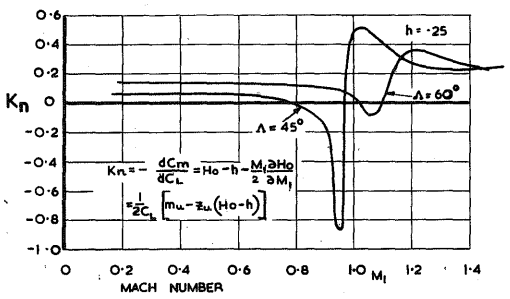

CONTRIBUTION OF THE WING FOR THE STATIC MARGIN.
DELTA PLANFORM.

FIG. 34.

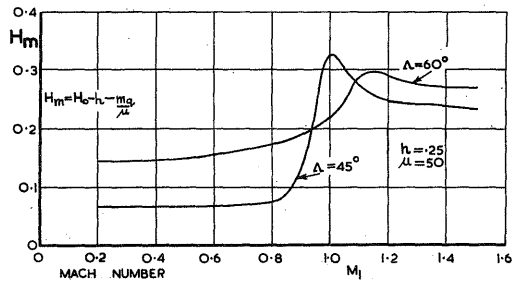

CONTRIBUTION OF THE WING TO THE MANOEUVRE MARGIN.
DELTA PLANFORM.

FIG. 35.

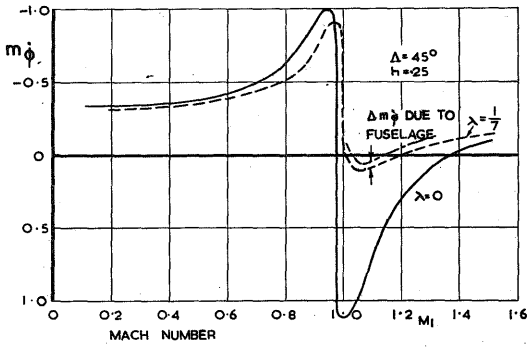

EFFECT OF TAPER ON THE DAMPING IN PITCH DERIVATIVE $m_{\dot{\phi}}$
DELTA PLANFORM.

FIG. 36.

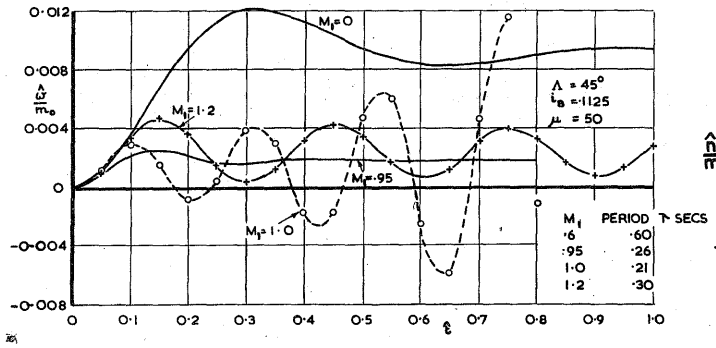

EFFECT OF MACH NUMBER ON RESPONSE.
DELTA PLANFORM.

FIG. 37

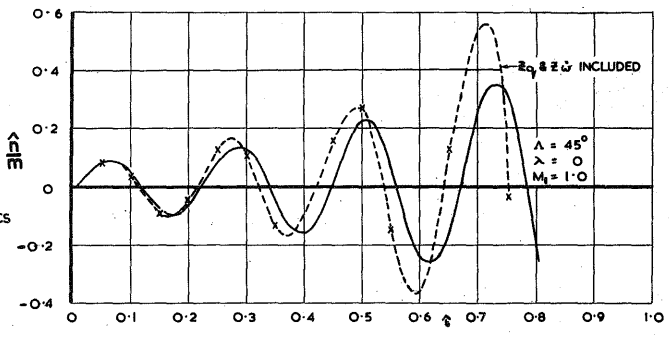

EFFECT OF NEGLECTING DAMPING IN LIFT DERIVATIVES.
DELTA PLANFORM.

FIG. 38.